



**NAVAL
POSTGRADUATE
SCHOOL**

MONTEREY, CALIFORNIA

THESIS

**NEAR FIELD SCANNING OPTICAL MICROSCOPY
(NSOM) OF NANO DEVICES**

by

Chun Hong Low

December 2008

Thesis Advisor:
Co-Advisor:

Nancy M. Haegel
James Luscombe

Approved for public release; distribution is unlimited

THIS PAGE INTENTIONALLY LEFT BLANK

REPORT DOCUMENTATION PAGE			Form Approved OMB No. 0704-0188	
Public reporting burden for this collection of information is estimated to average 1 hour per response, including the time for reviewing instruction, searching existing data sources, gathering and maintaining the data needed, and completing and reviewing the collection of information. Send comments regarding this burden estimate or any other aspect of this collection of information, including suggestions for reducing this burden, to Washington headquarters Services, Directorate for Information Operations and Reports, 1215 Jefferson Davis Highway, Suite 1204, Arlington, VA 22202-4302, and to the Office of Management and Budget, Paperwork Reduction Project (0704-0188) Washington DC 20503.				
1. AGENCY USE ONLY (Leave blank)		2. REPORT DATE December 2008	3. REPORT TYPE AND DATES COVERED Master's Thesis	
4. TITLE AND SUBTITLE Near Field Scanning Optical Microscopy (NSOM) of Nano Devices			5. FUNDING NUMBERS	
6. AUTHOR(S) Chun Hong Low				
7. PERFORMING ORGANIZATION NAME(S) AND ADDRESS(ES) Naval Postgraduate School Monterey, CA 93943-5000			8. PERFORMING ORGANIZATION REPORT NUMBER	
9. SPONSORING /MONITORING AGENCY NAME(S) AND ADDRESS(ES) National Science Foundation			10. SPONSORING/MONITORING AGENCY REPORT NUMBER DMR-0526330	
11. SUPPLEMENTARY NOTES The views expressed in this thesis are those of the author and do not reflect the official policy or position of the Department of Defense or the U.S. Government.				
12a. DISTRIBUTION / AVAILABILITY STATEMENT Approved for public release; distribution is unlimited			12b. DISTRIBUTION CODE	
13. ABSTRACT <p>This thesis aims to investigate the optical properties of nano-devices using the technique of Near-Field Scanning Optical Microscopy (NSOM). A unique set-up to perform Atomic Force Microscopy (AFM) and NSOM simultaneously in a scanning electron microscope (SEM) to collect spatially resolved luminescence and image transport on nano-scale structures, particularly nanowires, will allow direct determination of transport parameters, such as minority carrier mobility and diffusion length that are vital to the performance of optoelectronic devices.</p> <p>The work involves the development of a unique nano-scale imaging technique applicable to a wide range of structures. The main structures of interest in this thesis will be GaN nanowires. Instead of using a laser for generating charge for imaging, the e-beam from the SEM was used to generate localized charge for an NSOM probe to monitor the motion of the excess charge due to diffusion and/or drift via electron-hole recombination process. For the first time in this research, the author addressed numerous challenges such as the intricate NSOM technique to resolve sub-wavelength dimension measurements of the elements and determine optimized experimental parameters to compensate for the relatively low efficiency of NSOM optical collection. Of significance, transport imaging of 1-10 μm long GaN nanowires resulted in minority carrier diffusion lengths ranging from 1-2 μm.</p> <p>An initial experimental exploration was also conducted to determine the theoretical prediction of the unique transmission enhancement of Au nanobowties fabricated on luminescent GaAs heterostructure.</p> <p>The author will report the working principles, experimental procedures, optimal process parameters and the respective imaging results for assessing the properties of the nano-devices studied in this thesis work. Recommendations for future work pertaining to the augmentation of related NSOM work will also be made to ensure continued progress in this area of work.</p>				
14. SUBJECT TERMS Diffusion, Direct Transport Imaging, Minority Carrier Lifetime, Minority Carrier Mobility, GaN Nanowires, Nanobowties, Cathodoluminescence, Near field Scanning Optical Microscope, Atomic Force Microscope.			15. NUMBER OF PAGES 77	
			16. PRICE CODE	
17. SECURITY CLASSIFICATION OF REPORT Unclassified	18. SECURITY CLASSIFICATION OF THIS PAGE Unclassified	19. SECURITY CLASSIFICATION OF ABSTRACT Unclassified	20. LIMITATION OF ABSTRACT UU	

Standard Form 298 (Rev. 8-98)
Prescribed by ANSI Std. Z39.18

THIS PAGE INTENTIONALLY LEFT BLANK

Approved for public release; distribution is unlimited

**NEAR FIELD SCANNING OPTICAL MICROSCOPY (NSOM)
OF NANO DEVICES**

Chun Hong Low
Major, Singapore Armed Forces
B.Eng. (1st Class Hons), Nanyang Technological University, 2003

Submitted in partial fulfillment of the
requirements for the degree of

**MASTER OF SCIENCE IN COMBAT SYSTEMS SCIENCE AND
TECHNOLOGY**

from the

**NAVAL POSTGRADUATE SCHOOL
December 2008**

Author: Chun Hong Low

Approved by: Nancy M. Haegel
Thesis Advisor

James Luscombe
Co-Advisor

James Luscombe
Chairman, Department of Physics

THIS PAGE INTENTIONALLY LEFT BLANK

ABSTRACT

This thesis aims to investigate the optical properties of nano-devices using the technique of Near-Field Scanning Optical Microscopy (NSOM). A unique set-up to perform Atomic Force Microscopy (AFM) and NSOM simultaneously in a scanning electron microscope (SEM) to collect spatially resolved luminescence and image transport on nano-scale structures, particularly nanowires, will allow direct determination of transport parameters, such as minority carrier mobility and diffusion length that are vital to the performance of optoelectronic devices.

The work involves the development of a unique nano-scale imaging technique applicable to a wide range of structures. The main structures of interest in this thesis will be GaN nanowires. Instead of using a laser for generating charge for imaging, the e-beam from the SEM was used to generate localized charge for an NSOM probe to monitor the motion of the excess charge due to diffusion and/or drift via electron-hole recombination process. For the first time in this research, the author addressed numerous challenges such as the intricate NSOM technique to resolve sub-wavelength dimension measurements of the elements and determine optimized experimental parameters to compensate for the relatively low efficiency of NSOM optical collection. Of significance, transport imaging of 1-10 μm long GaN nanowires resulted in minority carrier diffusion lengths ranging from 1-2 μm .

An initial experimental exploration was also conducted to determine the theoretical prediction of the unique transmission enhancement of Au nanobowties fabricated on luminescent GaAs heterostructure.

The author will report the working principles, experimental procedures, optimal process parameters and the respective imaging results for assessing the properties of the nano-devices studied in this thesis work. Recommendations for future work pertaining to the augmentation of related NSOM work will also be made to ensure continued progress in this area of work.

THIS PAGE INTENTIONALLY LEFT BLANK

TABLE OF CONTENTS

I.	INTRODUCTION.....	1
A.	BACKGROUND	1
B.	MILITARY RELEVANCE	3
C.	THESIS OVERVIEW	4
II.	TRANSPORT IMAGING	7
A.	TRANSPORT THEORY	7
1.	Cathodoluminescence (CL)	7
2.	Transport Imaging	8
B.	NEAR-FIELD SCANNING OPTICAL MICROSCOPY (NSOM)	10
1.	Far-Field and Near-Field Microscopy	10
2.	History of NSOM	11
3.	Principles of NSOM	12
4.	NSOM Instrumentation and Setup.....	15
5.	Challenges of NSOM	16
III.	EXPERIMENTAL APPROACH.....	19
A.	CL EXPERIMENT	19
1.	Experimental Set-up	19
2.	Experimental Procedures.....	20
B.	AFM/NSOM EXPERIMENT.....	20
1.	Experimental Set-up	20
2.	Experimental Procedures.....	25
IV.	TRANSPORT IMAGING OF NANOWIRES	27
A.	GENERAL FEATURES OF GaN NANOWIRES	27
B.	CL IMAGING OF GAN NANOWIRES.....	28
1.	Panchromatic CL Imaging.....	28
2.	Monochromatic Intensity Mapping of Nanowire in ‘Spot-Mode’	30
C.	AFM/NSOM RESULTS	35
1.	PL-NSOM Experiment on GaAs Heterostructure	36
2.	AFM/NSOM Experiment on GaN Nanowires	36
V.	INITIAL INVESTIGATIONS ON AU NANOBOWTIES.....	47
A.	GENERAL FEATURES OF AU NANOBOWTIES	47
B.	AFM OF AU NANOBOWTIES	49
C.	NSOM OF AU NANOBOWTIES	52
D.	CHALLENGES FOR NSOM OF AU NANOBOWTIES	53
VI.	CONCLUSIONS AND SUGGESTIONS FOR FURTHER RESEARCH	55
A.	CONCLUSION	55
B.	SUGGESTIONS FOR FURTHER RESEARCH	56
1.	Overcoming Probe-Sample Charging “Drifting Effect”	56

2. Investigating Secondary Effects of the Enhanced Diffusion in GaN Nanowires.....	56
LIST OF REFERENCES.....	59
INITIAL DISTRIBUTION LIST	63

LIST OF FIGURES

Figure 1	(a) CCD Image of GaInP, and (b) CCD Image of Bulk GaAs.	9
Figure 2	Plot of 2-Dimensional Diffusion Intensity Mapping [from 9].	9
Figure 3	Schematic Illustration of Far- and Near-Field Microscopy.	11
Figure 4	Schematic Diagram for Obtaining Spatial Resolution of 500 Å Using a Scanning Optical Microscope (from [15]).....	12
Figure 5	NSOM Scan with an Externally Excited Generation Source.	14
Figure 6	Modes of Operation with NSOM.....	15
Figure 7	Schematic Diagram of a Typical NSOM Set-up.....	16
Figure 8	Probe Transmission at $\lambda = 633$ nm as a Function of Probe Aperture Diameter for Various Type of Probes (Pulled Probes, Double- etched Probes). The Dashed Curves Represent Theoretical Predictions while Solid Curves are Experimentally Obtained Results [from 17].	18
Figure 9	CL System and CCD Camera Integrated with a SEM.	19
Figure 10	Nanonics MultiView 2000 Scanner in the JEOL 840 SEM.....	21
Figure 11	(a) Anticlockwise from Top Left Hand Corner: Low Voltage Adaptor, HVPD for Upper Stage, SPM Controller, HVPD for Lower Stage and Counter and Power Supply for the APD. (b) The APD for Detecting Photons from the Fiber Probe During Measurements.	22
Figure 12	The Top (a) and Reverse (b) Views of the AFM/NSOM Probe Attached onto the MultiView 2000 Scanner.....	23
Figure 13	Schematic Diagram of the AFM/NSOM Probe.	24
Figure 14	Patented Tuning Fork Feedback Mechanism for AFM/NSOM Measurement (from [16]).....	24
Figure 15	(a) Tip Scanning (b) Sample Scanning.....	25
Figure 16	SEM Image of a 10 μ m Tapered GaN Nanowire.....	28
Figure 17	(a) SEM Image of a Pair of GaN Nanowires; (b) Panchromatic CL Image of the Same Wires.	28
Figure 18	(a) SEM Image of a 30 μ m GaN Nanowire; (b) Panchromatic CL Image of the Same Wire.....	29
Figure 19	Spatial Variation of Luminescence from GaN Nanowire in “Spot Mode” in Panchromatic Mode.....	30
Figure 20	CL Spectrum of GaN Nanowire.	31
Figure 21	(a) SEM Image of a 30 μ m GaN Nanowire; (b) Monochromatic CL Image at 360nm.	32
Figure 22	CL Intensity Map of GaN Nanowire in “Spot Mode” for $\lambda = 360$ nm....	32
Figure 23	a) SEM Image of a 30 μ m GaN Nanowire; (b) Monochromatic CL Image at 550 nm.....	33
Figure 24	CL Intensity Map of GaN Nanowire in “Spot Mode” for $\lambda = 550$ nm....	33
Figure 25	a) SEM Image of a 30 μ m GaN Nanowire; (b) Monochromatic CL Image at 660 nm.....	34
Figure 26	CL Intensity Map of GaN Nanowire in “Spot Mode” for $\lambda = 660$ nm....	34

Figure 28	NSOM Image of a 15-by-15 μm Scan which Shows the 2D Diffusion Effect from the PL Fixed Spot.....	36
Figure 29	AFM Image, NSOM Image and Luminescence Profile of a 5 μm GaN Nanowire.....	37
Figure 30	AFM, NSOM and Phase Image of 10 μm GaN Nanowire.....	37
Figure 31	The Luminescence Profile of the 10 μm GaN Nanowire as Measured across the Green Line Shown in Figure 30 above.....	38
Figure 32	3D Interpretation of NSOM Signal Superimposed on the Topography of the Wire 550 nm.....	38
Figure 33	NSOM on 5 μm GaN Nanowire, 10-by-10 μm Scan, at 1×10^{-8} A, 20.0 kV, 9000X.....	39
Figure 34	Semi-Log Plot of the Luminescence Intensity versus Distance for a 5 μm GaN Nanowire.....	40
Figure 35	Profile from a 5-by-5 μm AFM/NSOM Scan of a 10 μm GaN Nanowire.....	40
Figure 36	Semi-Log Plot of the Luminescence Intensity versus Distance for a 10 μm GaN Nanowire.....	41
Figure 37	Profile of a 20-by-20 μm AFM/NSOM Scan of a 15 μm GaN Nanowire at its Narrow End (~ 100 nm).....	42
Figure 38	Semi-Log Plot of the Luminescence Intensity versus Distance for a 10 μm GaN Nanowire at its Narrow End (~ 100 nm).....	42
Figure 39	Profile of a 20-by-20 μm AFM/NSOM Scan of a 15 μm GaN Nanowire at its Broad End (~ 500 nm).....	43
Figure 40	Semi-Log Plot of the Luminescence Intensity versus Distance for a 10 μm GaN Nanowire at its Broad End (~ 500 nm).....	43
Figure 41	Au Nanobowties Array Fabricated on a GaAs Heterostructure with Au Strips of 10 μm Pitch to Demarcate the Locations of Nanobowties at 10 μm Intervals along Each Strip (Image Captured Using NovelX mySEM). This is the Actual Sample Used for this Thesis Work.....	47
Figure 42	A Pair of Au Nanobowties with 50 nm Gap (Image Captured Using NovelX mySEM).....	48
Figure 43	AFM Image of a Pair of Au Nanobowtie and its Profile Measurement.....	49
Figure 44	A Pair of Au Nanobowties with a 45 nm Gap Measured by AFM and its Corresponding Topography Profile.....	50
Figure 45	1 μm by 1 μm AFM Scan of a Pair of Nanobowties with (a) SEM Beam Off and (b) SEM Beam On.....	51
Figure 46	A Pair of Au Nanobowties Measured with a 10 nm AFM Probe.....	51
Figure 47	(a) The E-beam was Placed (with a Cross-hair) at Close Proximity to the Gap of the Nanobowtie so as to Determine Any Optical Enhancement Effects; (b) The Location of the E-beam after a Complete Scan will not have the Proximity for Optical Field to Reach the Gap.....	52

ACKNOWLEDGMENTS

The author would like to express his sincere gratitude to his adviser Professor Nancy Haegel for her encouragement, advice, suggestion and valuable guidance throughout the course of this master thesis. She has proven to be an excellent mentor by being patient, supportive and appreciative of all that was accomplished during this period. The learning experience acquired during these twelve months has been enriching and fruitful. I would also like to thank my co-advisor, Prof Luscombe for his efforts in ensuring the high quality of this thesis.

My appreciation extends to collaborators Dr. A. Alec Talin and Dr. Thomas Boone for the GaN nanowires and Au nanobowties samples respectively, without which this thesis work will never be in existence. Special thanks to Andrey Ignatov, Rimma Dechter, Abraham Israel and Hitesh Mamgain of Nanonics for the enriching scientific exchange experience in Jerusalem, Israel. Additionally, I appreciate Dr Maozi Liu's kind gesture for the use of his high-resolution AFM system at Agilent Technologies.

I wish to thank Mr Sam Barone for all his kind help in all aspects especially his expertise in coupling of optical fibers and thanks to all who have contributed in one way or another to make this thesis a success. This work is supported by the National Science Foundation through Grant DMR-0526330.

To my wife, Shirley, thank you so much for your unwavering support and understanding for the long hours away from you all these while in my work and I dedicated this success to you.

THIS PAGE INTENTIONALLY LEFT BLANK

I. INTRODUCTION

There's Plenty of Room at the Bottom

Richard Feynman

A. BACKGROUND

Nanotechnology is no longer the field of speculation. Since its early developments in the 1980s, it has become increasingly important in a range of materials and applications. Existing applications include novel optoelectronic devices such as photonic crystals and quantum dots, and carbon nanotubes for low energy consuming displays. At the same time, there is wide agreement that many new applications and devices will affect future electronics, medical and environmental areas. Most research in nanotechnology began from the study of nano-structures and their properties before fabricating them into useful nano-devices.

“Nano” is defined as a structure at the atomic and molecular scale. It is commonly known to be concerned with structures of the order of 100 nm or smaller. There is a progressive interest in 2D, 1D and 0D quantum wells, wires and dots, as the phenomenon of electronic confinement makes them interesting for optoelectronic applications.

While much research aims to develop innovative and effective growth of nano-structures like wires as well as controlling the direction of growth [1], it is also important to characterize the optical properties of these devices which are critical in identifying their applications in optoelectronic devices like chemical and biological sensors, photovoltaic and nano-electronics. The progression in nanotechnology fabrication techniques has also yielded a great demand for instrumentation that provides the high resolution imaging required. Thus, this thesis seeks to study the unique transport properties of several nano-devices such as nano-wires and nano-bowties by developing a new optical characterization technique optimized for nano-scale measurements.

The technique of transport imaging [2,3] has demonstrated the ability to characterize minority carrier transport properties (diffusion and drift) in nano-structures. An optical microscope was installed within a Scanning Electron Microscopy (SEM) and used to image the spatial distribution of luminescence created by an e-beam point source excitation and diffusion and/or drift effects. This approach effectively measures the minority carrier diffusion length (in the absence of an electric field). This work creates the stepping stone to extend the idea of transport imaging to the nano-scale using the technique of Near-Field Scanning Optical Microscopy (NSOM) for the direct characterization of carrier diffusion in nano-devices.

Determining the spatial variation of luminescence with a standard Optical Microscope (OM) imposes a resolution limit determined by far-field optics. Hence, utilizing the approach of direct imaging of electron/hole recombination via an OM and a high sensitivity charge coupled device, coupled to a SEM to capture spatial information about the transport behavior in luminescent solid state materials will be infeasible. A unique set-up incorporating the application of Atomic Force Microscopy (AFM), Near-Field Scanning Optical Microscopy (NSOM) and SEM in one integrated system will be used instead. The SEM enables the generation of a localized e-beam charge onto the luminescent sample of interest in a similar fashion as the method used in [2,3] and using a AFM-NSOM tip from Nanonics to scan and pick up the topography and optical signal (from the electron-hole recombination process) simultaneously. Previously, the charge motion could be imaged spatially by an optical microscope (OM), but as the structures of interest will be of nano-scale dimensions of sub-wavelength, NSOM is used to overcome diffraction-limited resolution. This was attempted on ZnO nano-wires done in an earlier thesis [4]. Hence, this thesis will take this to another level by demonstrating NSOM operation in a SEM to collect spatially resolved luminescence and to image transport on nano-scale structures, particularly nanowires, in 1-D. This will allow direct determination of transport

parameters, such as minority carrier mobility and diffusion length that are vital to the performance of LEDs, lasers and bipolar devices.

The primary goal of the work is the development of a unique nano-scale imaging technique applicable to a wide range of structures. Two main structures of interest in this thesis will be GaN nano-wires and Au nano-bowties. Numerous challenges such as mastering the intricate NSOM technique to resolve sub-wavelength dimension measurements of the elements and determine optimised experimental parameters to compensate for the relatively low efficiency of NSOM optical collection were addressed for the first time in this research. The details of the technique and optimal experimental parameters will be discussed in the subsequent chapters of this thesis.

B. MILITARY RELEVANCE

Nanotechnology has been a buzzword for decades since its inception and military nanotechnology can be considered as an opportunity in defense evolution. With nanotechnology, the nano-inspired evolution and transformation of defense capability offers the potential for military applications that are far-reaching and unprecedented. These include not only new, previously uncharted areas of application, but also the potential for higher density devices with corresponding size and weight savings, as well as cost containment.

The defense industries as well as government have long been pursuing the basic research for potential applications in warfare [5]. Recent demonstration of the use of nanotechnology-enhanced systems [6] in modern conflicts like Operation Iraqi Freedom has reiterated the importance of keeping pace with nanotechnology research and development to maintain the technological edge. A fine example will be the application of lightweight high-strength nano-composites to increase the survivability of Marine Corps' M1A1 Abrams tanks and light armoured vehicles.

Today's "small" is considered the past "big". In the most conventional area of weaponry, nanotechnology's ability to miniaturize present weaponry [7] with

enhanced firepower, computing power and precision with minimal power consumption provides increase firepower capacity with the same payload for every platform.

Myriad of other relevant military applications of nanotechnology in areas such as sensors, C4ISR, countermeasures and portable power also add to the increased capabilities of today's war fighters. Sensors represent one of the largest potential uses of nanotechnology with the emergence of mini-UAVs, mini-USVs and other miniaturised unmanned platforms anticipated for future conflicts. These include imaging sensors, chemical sensors and bio-sensing and other areas in which nano-photonics devices are used including computing systems and microprocessors, data storage, and optical signal processing.

Concurrently, one of the greatest challenges in the field of nanotechnology is the ability to optically image nano-structures at high resolution and characterize devices to obtain the relevant electro-optical properties. As all nano-devices utilize nano-structures like nano-wires as their building blocks, this thesis aimed to study the optical characteristics of GaN nano-wires and Au nano-bowties. Due to the size of these elements being diffraction-limited for OM to be employed, a major part of the measurements were done via the technique of NSOM. This thesis work attempts to advance some of the basic characterization research required to support the advance of nanotechnology. Similar to defense interest in the fundamental research that led to revolutionary applications in lasers, integrated circuits and the internet, modern military programs are investing today in nanotechnology.

C. THESIS OVERVIEW

This thesis begins with a brief introduction on the emergence of nanotechnology and its military relevance. Chapter II then provides a literature research of the technique of transport imaging and a detailed description of NSOM. This chapter will cover the theory of transport imaging, the principles of NSOM and the features of nanostructures like nano-wires and nano-bowties.

Chapter III will describe the experimental approach on imaging nano-structures using the unique integrated system of AFM and NSOM in a SEM. Different samples, namely GaN nano-wires and Au nano-bowties, were measured to study the effects of carrier diffusion and optical properties. Experimental conditions and parameters will be the key issues to be explored as part of this thesis to obtain optimal results. Optical properties such as the diffusion lengths and luminescence properties will be reported.

Chapter IV reports the imaging results of the experiments and significant findings of NSOM measurements of GaN nanowires luminescence and the determination of minority carrier diffusion length. Relationship between the size of the nanowires and the effects of diffusion will also be reported.

Chapter V describes an initial study on Au nanobowties for the investigation of a possible optical field enhancement in between a pair of nanobowties. While no major finding has been found to date, recommendations on overcoming the technical challenges faced offer great potential in this work.

Finally, Chapter VI will conclude and summarise the project findings and conclusions. Suggestions for future work will also be discussed.

THIS PAGE INTENTIONALLY LEFT BLANK

II. TRANSPORT IMAGING

A. TRANSPORT THEORY

1. Cathodoluminescence (CL)

CL is a conventional method used in the characterization of luminescence in semiconductors. The main principle of CL depends on the recombination of electron-hole pairs after the process of releasing of valence band electrons to the conduction band on the absorption of energy from incident electrons. On recombination, photons may be emitted and their wavelength will depend on the material involved and can be derived from the relation:

$$E_f - E_i = \frac{hc}{\lambda}$$

where E_i and E_f are the initial and final energies of the electron. The luminescence may involve band edge states or it may involve recombination at defects or impurities, in which case $E < E_{\text{gap}}$.

Generally, the electron beam energy used in CL measurements ranges from a few to 30 keV. In comparison with PL, a CL electron of around 30 keV is capable of generating thousands of electron-hole pairs. This number, G (number of electron-hole pairs generate per incident beam electron), can be calculated as [8]:

$$G = \frac{E_b(1 - \gamma)}{E_i}$$

where E_b and E_i are the electron beam and ionization energies of the electron for the formation of electron-hole pair, and γ is fractional electron beam energy loss

due to backscattered electrons. At the same time, the depth of electron penetration, R_e , is dependent on E_b and can be calculated using the following relationship:

$$R_e = \left(\frac{k}{\rho}\right) E_b^\alpha$$

where ρ is the density of the material, and k and α are parameters related to the e-beam energy and atomic number respectively.

2. Transport Imaging

While CL is able to characterize optical properties of luminescent materials, it does not maintain the spatial information in its measurement. During the conduct of a CL intensity mapping measurement, all light captured is attributed to all the points of excitation along where the element is measured. Hence, the same amount of excitation was placed on every part of the element and the intensity of the resultant light is measured. This does not capture the effects of transport phenomenon. Only with the inception of the technique of transport imaging, can the spatial information of a fixed point of excitation on an element be determined. This technique allows for a highly controllable localized charge generation process to obtain imaging at high spatial resolution and can be employed on wide band-gap as well as multilayer materials. Transport imaging is the technique of imaging both the motion and recombination of charge in luminescent semiconductors. This technique enables the extraction of transport parameters such as the minority carrier diffusion length [3], which is critical to bipolar device operations like solar cells and transistors. This has been done by D. R. Luber et al. in demonstrating the measurement of minority carrier diffusion length of a heavily doped GaAs double heterostructure using an integrated system of a OM and CCD camera in a SEM. Examples of images obtained for a brief study on possible substrates for the fabrication of nano-devices are shown in Figure 1. Figure 2 shows the logarithmic plot of the diffusion intensity distribution captured by this technique for semiconductor heterostructures with varying diffusion lengths.

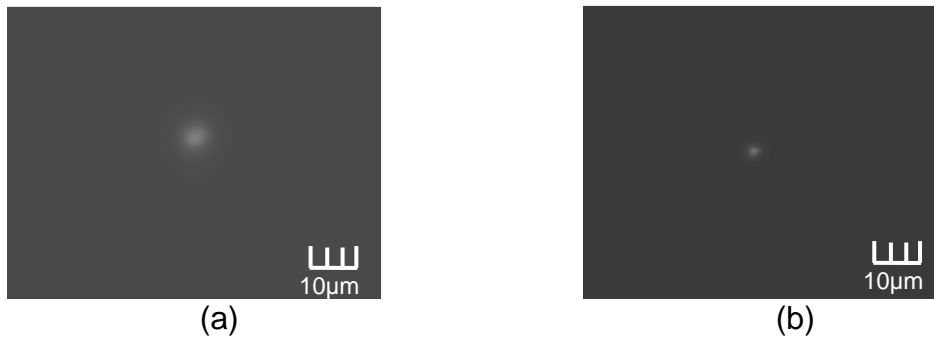


Figure 1 (a) CCD Image of GaInP, and (b) CCD Image of Bulk GaAs.

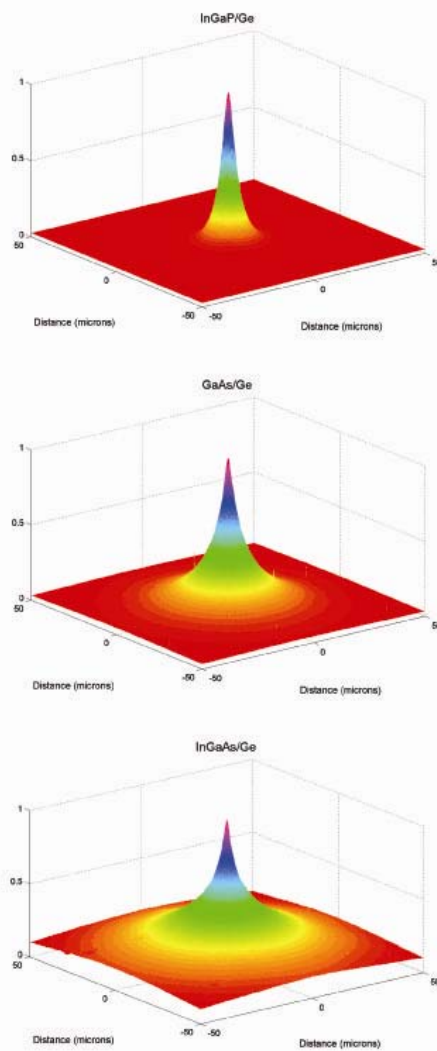


Figure 2 Plot of 2-Dimensional Diffusion Intensity Mapping [from 9].

Similarly, a direct transport imaging technique designed for planar structures [2] has been demonstrated in a SEM and an OM with a high sensitivity charge coupled device. This thesis, however, will attempt to take transport imaging technique to another level by imaging the effects of transport at near-field using NSOM in a SEM. The effects of transport and diffusion will be determined experimentally by measuring the intensity distribution within structures like nano-wires. While the above-mentioned technique enables the measurement of transport properties for planar structures through OM imaging, NSOM will enable transport imaging at near-field to obtain the spatial distribution of optical signal from a fixed source of structures that are sub-wavelength in dimensions.

B. NEAR-FIELD SCANNING OPTICAL MICROSCOPY (NSOM)

1. Far-Field and Near-Field Microscopy

The late Ernst Karl Abbe was the first to approximate the diffraction limit [10] to be:

$$d = \frac{\lambda}{2 \sin \theta}$$

where d is distance between 2 objects, λ is wavelength of the incident light, and 2θ is the angle through which the light is collected.

As such, the resolution between objects in a standard far-field optical microscope is d . For instance, visible light is in the range of 400 – 700 nm, and with 400 nm being the smallest wavelength, the best resolution achievable (with θ at 90°) is 200 nm. Anything below this size is considered as diffraction-limited and unable to be resolved by far-field imaging.

However, with the advancement of nano-fabrication techniques and the fast development of nanotechnology, nano-scale characterization requires technology imaging below the wavelength of incident or emitted light. For instance, nano-structures such as nanowires, can be less than 100 nm in

diameter. The emergence of near-field optics opens the doors to sub-wavelength resolution. With the introduction of Near-Field Scanning Optical Microscopy (NSOM), the limitation of diffraction is eliminated, and higher resolution of luminescence is achievable through the collection of light in near field. The near-field region is defined as the region in space where the effects of evanescent waves are not negligible.

The key principle behind collection at near field is by passing light through an aperture of sub-wavelength diameter to illuminate the sample of interest that is placed within its near field ($r \ll \lambda$). Instead of depending on the wavelength of the incident or emitted light, the aperture size becomes the determining factor for the resolution limit.

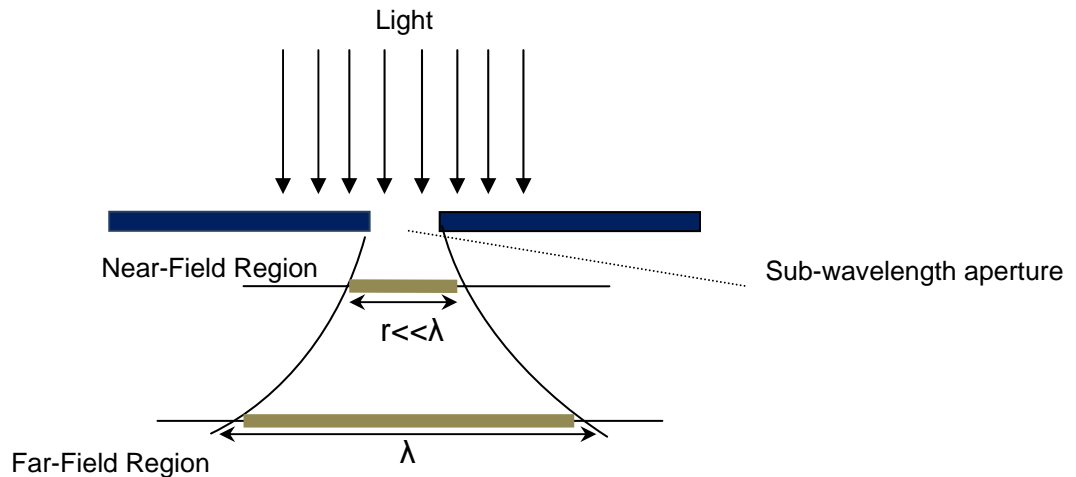


Figure 3 Schematic Illustration of Far- and Near-Field Microscopy.

2. History of NSOM

The idea of NSOM was first promulgated by E.H. Synge in the late 1920s. He designed an experiment with the concept of passing light through a small aperture of sub-wavelength diameter [11,12]. Besides Synge, other scientists like J.A. O'Keefe and E.A. Ash and G. Nichols conducted their own experiments with acoustics and microwaves in 1956 [13] and 1972 [14], respectively. It was not

until 1984 that A. Lewis et al., [15] proved the viability of NSOM in the optical part of the spectrum. Apertures of dimensions 80 – 2400 Å were fabricated via e-beam etching and a Leitz Ortho-plan microscope with a tungsten filament emitting at around 5800Å was used to capture the images on Polaroid films. Experimental results showed that sub-wavelength spatial resolution of 500 Å is achievable. Figure 4 below shows a schematic diagram of a possible set-up for such sub-wavelength measurements.

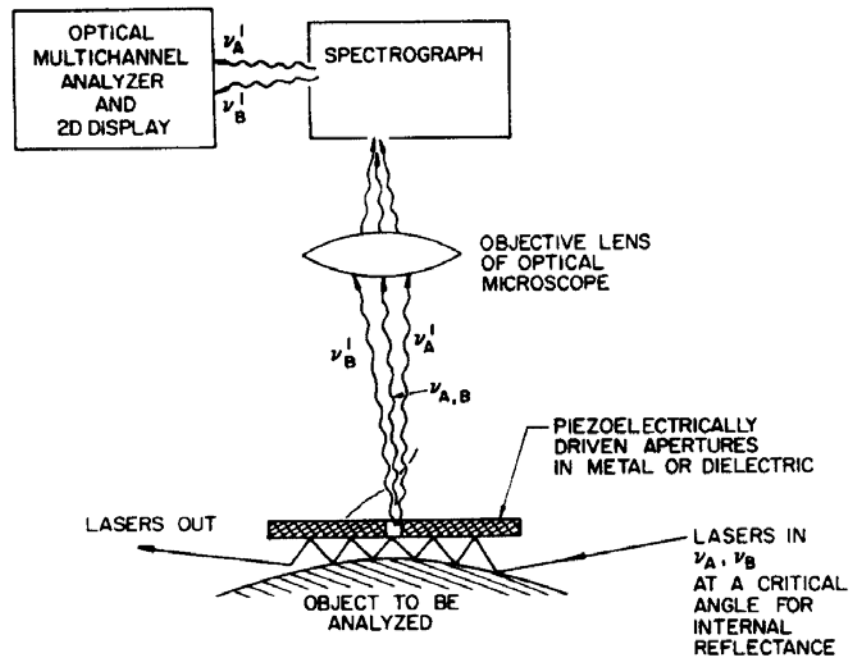


Figure 4 Schematic Diagram for Obtaining Spatial Resolution of 500 Å Using a Scanning Optical Microscope (from [15])

3. Principles of NSOM

As the name suggests, NSOM requires bringing a point source of light like the aperture of a probe, in close proximity (but not in contact) to the surface of the sample of interest to be imaged and then collecting the optical signal from the surface of the sample. NSOM is based on the detection of non-propagating evanescent waves in the near-field region. In general, it measures a spatially

resolved impedance of the sample of interest by scanning a tip of an evanescent wave probe toward the surface of the sample within a sensing distance in near-field. This is achieved through generating an evanescent wave with at least one time varying amplitude and a time varying phase, measuring the change in resonant frequency of the evanescent wave probe over time as well as the change in quality factor of the probe and determining the impedance of the sample based on these changes.

In order to achieve an optical resolution better than the diffraction limit, an optical fiber probe of sub-wavelength aperture will be brought within the near-field region and used like a waveguide. As mentioned earlier, near-field is defined as the region that is very much less than the wavelength of the incident light (usually on the order of 1 nm). The aperture size will determine the luminescence resolution of each set-up. In the case of an externally excited source, the resolution will be defined by the size of the light source used.

An avalanche photodiode (APD) with a photon counter will then be used to amplify the collected light from the other end of the fiber to measure the relative intensity of the measurement. The varying intensity will then translate to the NSOM images in a software program. The sources of light used in NSOM vary and depend on the nature of the particular experiment. Typically, laser light is fed to the aperture via a tapered optical fiber coated with gold to excite the luminescence. Alternatively, an independent source of light such as a laser beam may be used to excite the area of interest on the sample and the collection of the optical signal will be done by scanning the NSOM probe across. A unique excitation source would be the e-beam from a SEM. In this thesis, the e-beam that ranges from 10-30 keV of accelerating voltage from an SEM is utilized as the excitation source for NSOM measurement. A schematic illustration is shown in Figure 5.

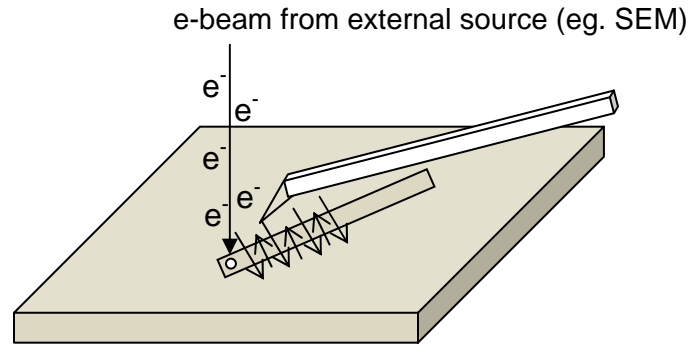


Figure 5 NSOM Scan with an Externally Excited Generation Source.

In general, feedback mechanisms are used in controlling the distance between the aperture and the sample surface at the sub-nanometer scale required. Two of the more commonly employed feedback mechanisms are: Normal Force Feedback and Shear Force Feedback. The former utilizes AFM cantilevers with apertures or tapered optical fibers with standard feedback modes like contact and tapping mode, while the latter makes use of the difference in amplitudes of a tuning fork oscillation, which depends on the tip-surface distance.

There are four possible modes of operation with NSOM [16]: Transmission Mode, Reflection Mode, Collection Mode and Illumination/Collection Mode (Figure 6).

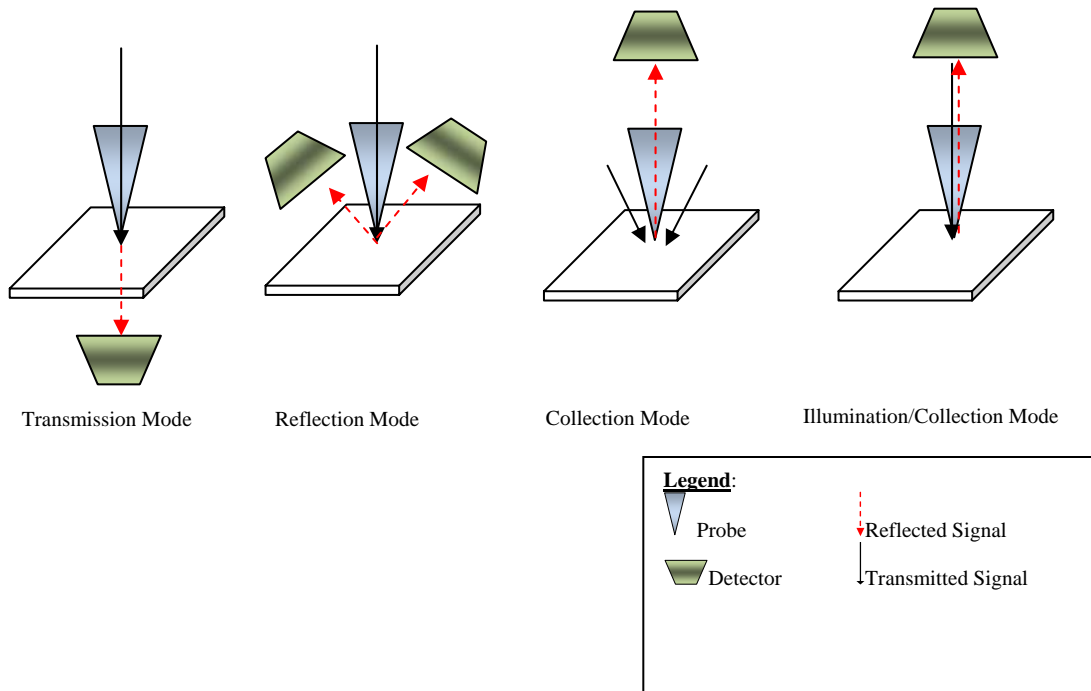


Figure 6 Modes of Operation with NSOM.

In both transmission and reflection mode imaging, the probe illuminates the sample but the optical signal through the sample is collected and measured for transmission mode, while the reflected signal is collected and measured for reflection mode. Collection mode imaging illuminates the sample with a macroscopic light source and collects the signal from the sample surface via a probe. Finally, in illumination/collection mode imaging, light is both incident through the probe as well as collected via the probe for the reflected or emitted signal.

4. NSOM Instrumentation and Setup

The primary components of an NSOM apparatus consist of the light source, sample, scanning tip, feedback mechanism, optical detector (such as an APD) and a piezoelectric stage. In this thesis we will focus on the SEM e-beam as the external excitation source. Fiber optic AFM/NSOM scanning tip by

Nanonics will be the only type of NSOM tips used in this work and will be discussed in the next chapter. A schematic of a standard NSOM setup is depicted in Figure 7.

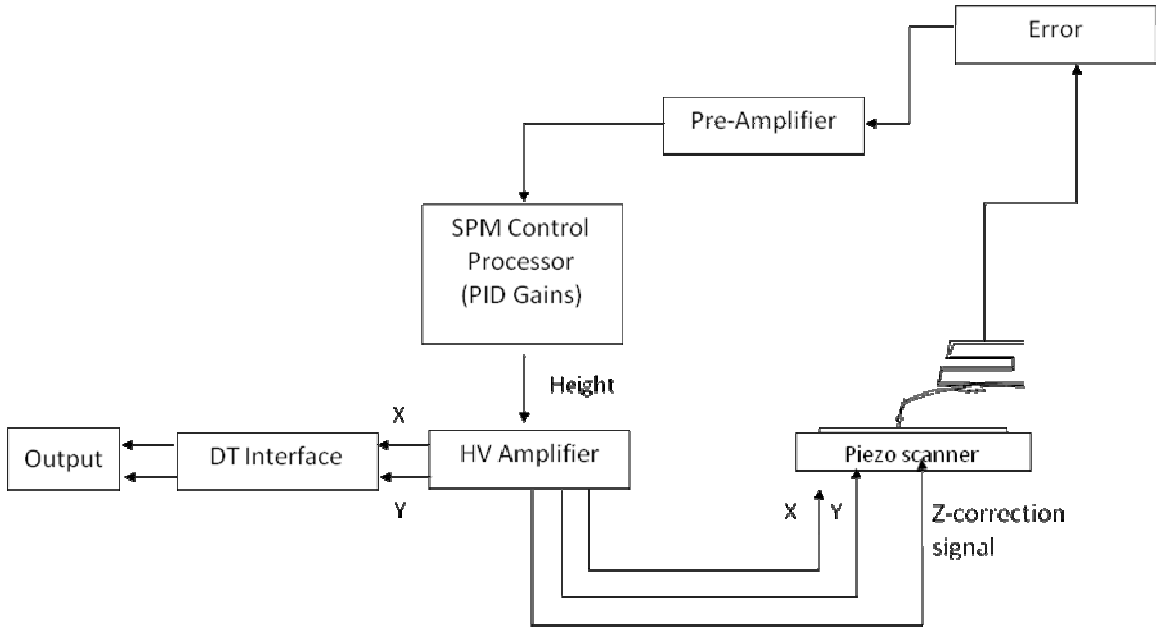


Figure 7 Schematic Diagram of a Typical NSOM Set-up.

5. Challenges of NSOM

While NSOM exhibits extraordinary advantages in near-field optics measurement, there are many challenges that the operator has to overcome in this field of work. First, the working distance of NSOM is very small and hence, a very narrow field of view. This will be a tough challenge for very small structures fabricated on a large sample without guiding features to locate the structures of interest. As such, it is recommended that all structures to be studied be fabricated (whenever possible) with guiding features on the sample to mark them out significantly for easy locating. Second, NSOM scans usually take a long period of time especially for large samples and/or high resolution imaging. This is a drawback which can only be improved over time with better equipment and the

only mitigating approach is to locate structures using lower resolution before conducting high resolution scans across them. Third, due to the need for the probe to be at near-field, high quality feedback mechanisms have to be employed. As such, normal force feedback mechanism using an AFM cantilever is a better option vis-à-vis the shear force mechanism because of the higher level of repeatability and stability in the former.

Lastly, there is the trade-off issue of obtaining high-resolution imaging with lower efficiency of luminescence collection via probes of smaller aperture or low-resolution imaging with higher efficiency for luminescence collection using probe of larger apertures [17]. A brief illustration on the relative effects of the size of the aperture to the efficiency of optical collection can be shown by the experimental results from Figure 8. For instance, with a D^4 dependence, reduction of collecting aperture from 250 to 100nm is predicted to decrease efficiency by a factor of ~40. Thus, a balance has to be struck for optimal results. These limitations present significant challenges for transport imaging at the nano-scale, but the work presented will demonstrate, for the first time, the potential to overcome these limitations to obtain direct information on minority carrier diffusion within individual GaN nano-wires.

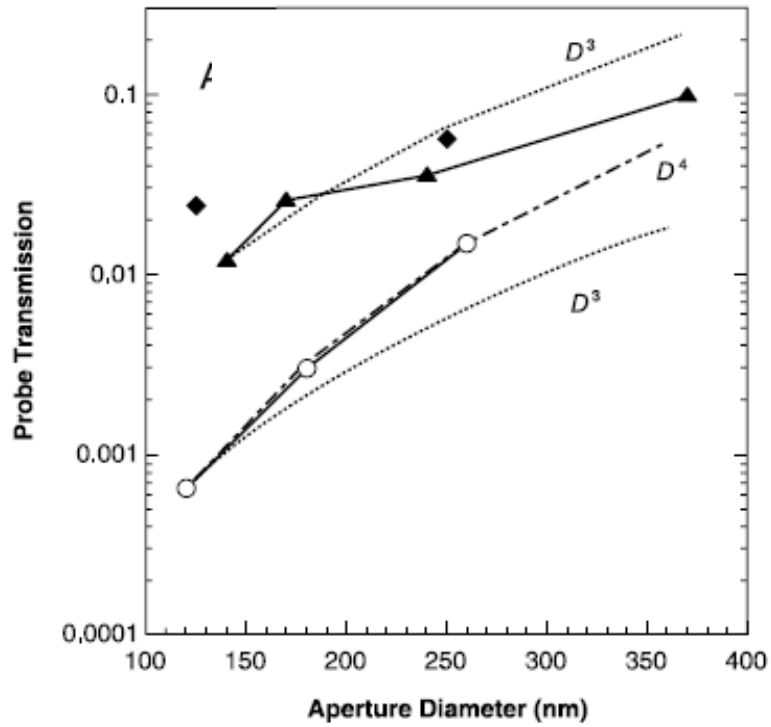


Figure 8 Probe Transmission at $\lambda = 633$ nm as a Function of Probe Aperture Diameter for Various Type of Probes (Pulled Probes, Double-etched Probes). The Dashed Curves Represent Theoretical Predictions while Solid Curves are Experimentally Obtained Results [from 17].

III. EXPERIMENTAL APPROACH

A. CL EXPERIMENT

1. Experimental Set-up

While NSOM is the key experimental technique to investigate the transport properties of nano-devices in this thesis, CL experiments are crucial in determining the spectral distribution as well as the intensity of photon emission from the structures under study. The CL system used in this study is from Gatan (previously Oxford Instruments) and it has a retractable arm with a parabolic collecting mirror that can be inserted into the SEM chamber. Externally controlled mirrors allow the system to be operated in panchromatic as well as monochromatic mode for imaging, in addition to spectroscopy. The monochromator is 1/3 m with a grating of 1200 l/mm. Additionally, another unique feature of the CL set-up in this work involved an attachment of an OM with a Si CCD array camera to capture images of the effects of CL. Figure 9 shows the attachment of the Gatan CL system and SI CCD camera to the JOEL SEM.

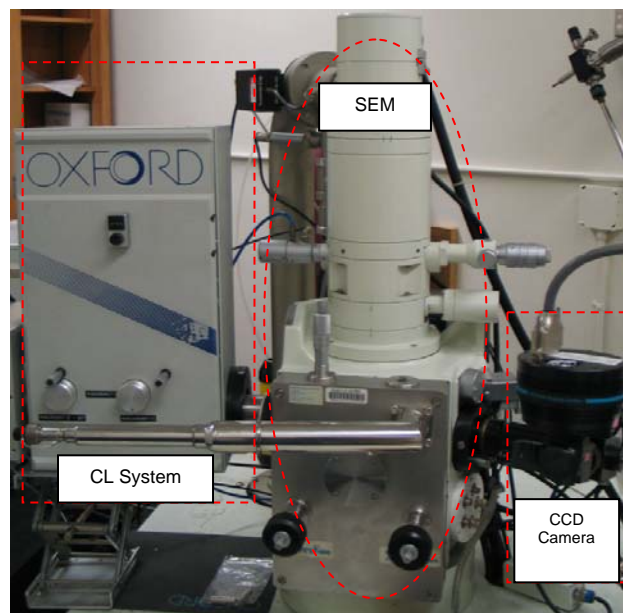


Figure 9 CL System and CCD Camera Integrated with a SEM.

2. Experimental Procedures

The CL system's main purpose is to determine the spectroscopy of the GaN nano-wire luminescence. It is first used to determine the spectrum and relative luminescence from the wire. The GaN nano-wires studied in this thesis are between 1 – 30 μm in length and 100 – 500 nm in diameter. Understanding the spectrum of the nano-wires allowed us to differentiate the spectral characteristics of nano-wires and the substrates that they are grown or deposited on.

Then, CL 'spot mode' was performed along the wires for an intensity mapping of the luminescence of the wire at different wavelengths in monochromatic mode. This determined the relative intensities and responses from the wires at different wavelengths. The results and analysis will be discussed in subsequent chapters.

B. AFM/NSOM EXPERIMENT

1. Experimental Set-up

The experimental set-up in this work is unique and exceptional. It involves the integration of an AFM/NSOM scanner within a SEM, for the main reason of being able to use the SEM for easy locating of sample structures and to use the e-beam of the SEM as the high resolution carrier generation source for NSOM measurement. The benefits of this include 1) being able to decouple the excitation from the light collection and 2) utilizing the potentially small generation spot provided by e-beam optics. Many standard scanning probe technologies are not compatible with the requirements of these unique experiments. Most of them employ straight optical fibers which would obstruct the e-beam's path from the top of the SEM to impinge onto the surface of the sample for NSOM experiment. Also, most scanning probe microscopy (SPM) systems are based on a cylindrical piezo device that is held perpendicularly to the sample or probe to be scanned.

This results in blocking the top, bottom or both simultaneously and hence, prevents the flexibility of integrating the many useful aspects of it into standard optical, electron and ion-beam systems.

Thus, this thesis work utilizes Nanonics' MultiView 2000 AFM/NSOM System. This specially designed system allows for an integrated AFM/NSOM scan simultaneously in a SEM. The MultiView 2000 AFM/NSOM scanning stage is shown in Figure 10. Special customization has been done to allow for such integration so that the measurement signals within the SEM can be piped out to the actual control equipment outside the SEM.

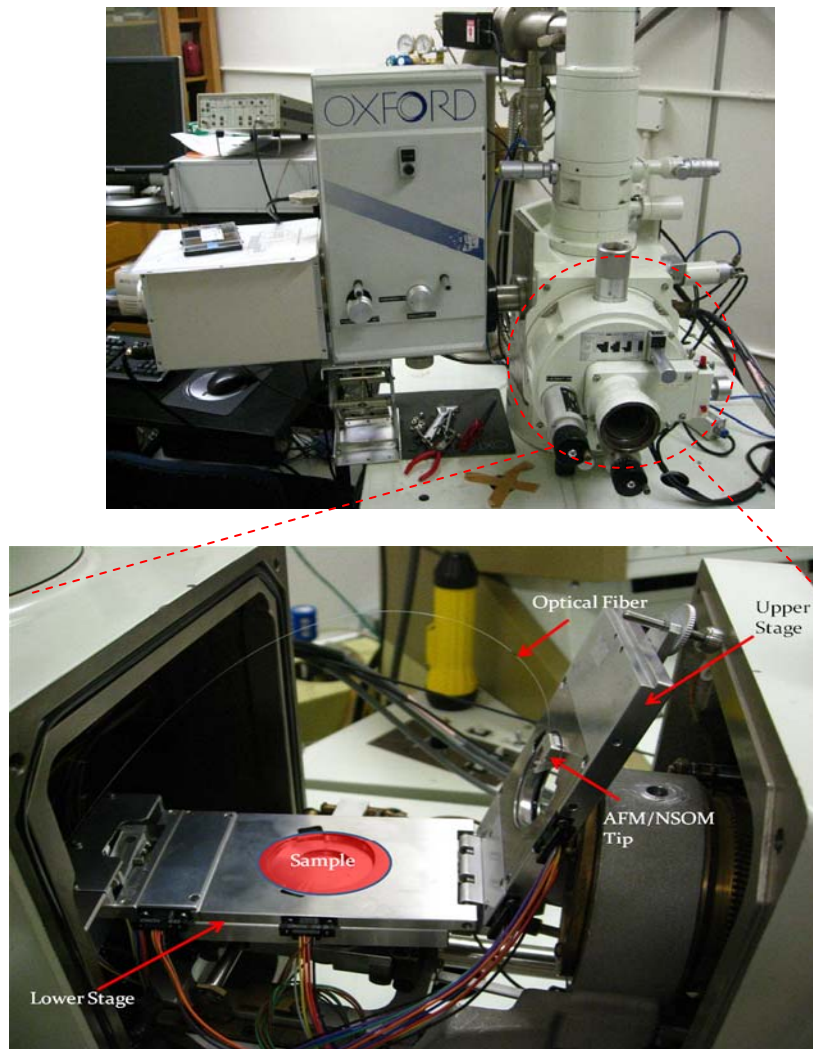


Figure 10 Nanonics MultiView 2000 Scanner in the JEOL 840 SEM.

Other components of this set-up include the High Voltage Piezo Drivers (HVPD) that control the displacement of the stage, as well as the probes in three dimensions, the SPM controller which controls the Proportional, Integration, and Differential (PID) parameters for adjusting the sensitivity of the scanning probe measurements, the Low Voltage Adaptor that allows for the selection of sample or tip scanning and Z-feedback component, and lastly the APD for detection of photon count-rate in NSOM measurements. These components (Figure 11) are all cabled to the MultiView 2000 in the SEM.



Figure 11 (a) Anticlockwise from Top Left Hand Corner: Low Voltage Adaptor, HVPD for Upper Stage, SPM Controller, HVPD for Lower Stage and Counter and Power Supply for the APD. (b) The APD for Detecting Photons from the Fiber Probe During Measurements.

The scanning stage makes use of what Nanonics termed as 3D Flat Scanning Technology such that the flat scanners are based on the same scanning mechanism as all AFM piezo scanners. Hence, this scanner can provide the same scanning mechanism, not only for standard AFM in the X and Y scan directions, but also in a large Z-scan range of 70 μm . This enables users to investigate structures of high topography and deep trenches.

The scanning probe (See Figure 12 for physical images of the probe on a scanner and Figure 13 for a schematic diagram of the probe) that is used in this thesis work is unique and worth reviewing. It is an improved version of probes as compared to those used in previous work. As the previous style of probes were magnetically mounted onto the scanner and had caused strong tip-sample astigmatism that affects the image due to interaction of the e-beam with the magnetic field, the newly designed tips are mechanically mounted and hence, eliminates the strong astigmatism of the image experienced in earlier work. The probe is an integrated AFM/NSOM probe that utilizes a patented tuning fork feedback mechanism (See Figure 14). While the use of tuning fork as part of SPM was filed as a patent (US Patent 5641896) by K. Karrai and M. Haines in 1995, Nanonics extends this invention through the use of proprietary, simple mounting techniques that maintain resonance frequencies and Q factors for tuning fork feedback [18] without the geometrical restrictions that Karrai had for his straight near-field optical/AFM elements.

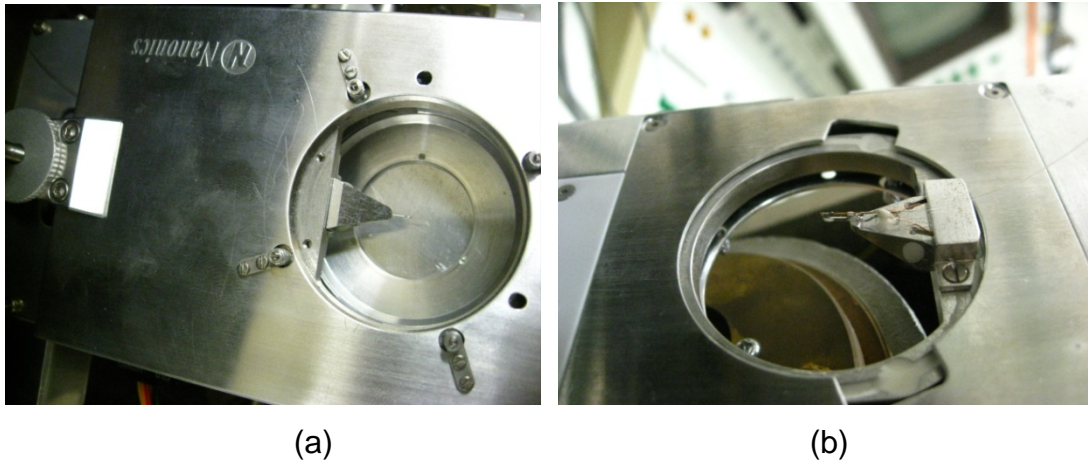


Figure 12 The Top (a) and Reverse (b) Views of the AFM/NSOM Probe Attached onto the MultiView 2000 Scanner.

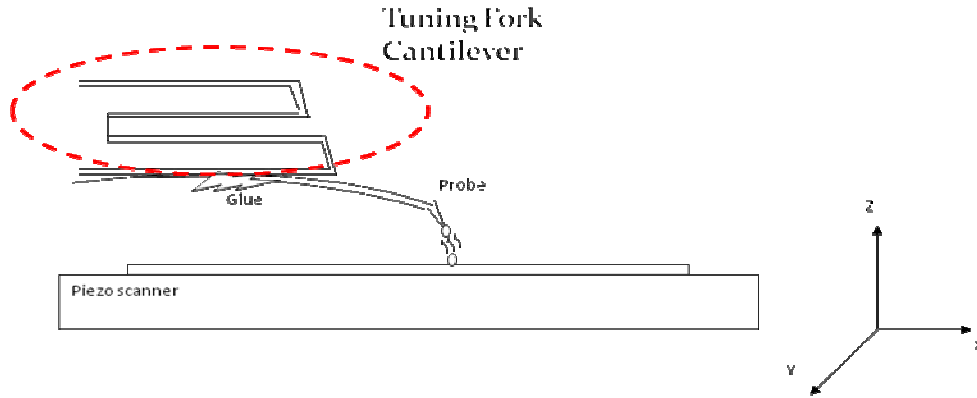


Figure 13 Schematic Diagram of the AFM/NSOM Probe.

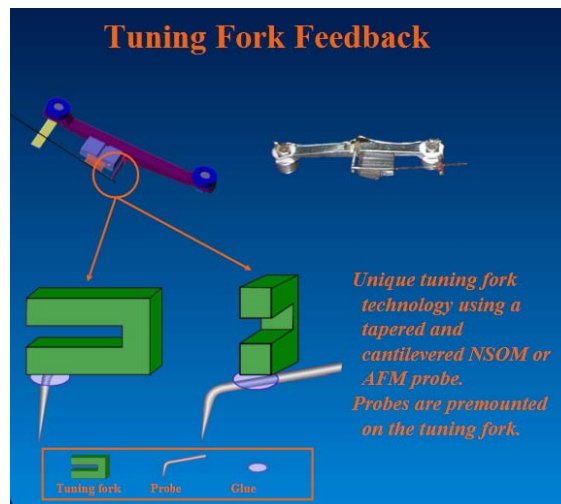


Figure 14 Patented Tuning Fork Feedback Mechanism for AFM/NSOM Measurement (from [16])

In addition to the unique tuning fork feedback mechanism, it is significant to note that only Nanonics' MultiView 2000 scanner can allow for scanning either by moving the sample or the probe (See Figure 15) on a single platform. This is an important application for NSOM experiments requiring the scanning of the probe with a fixed light source to map the optical properties spatially on the sample as the collecting probe scans across it.

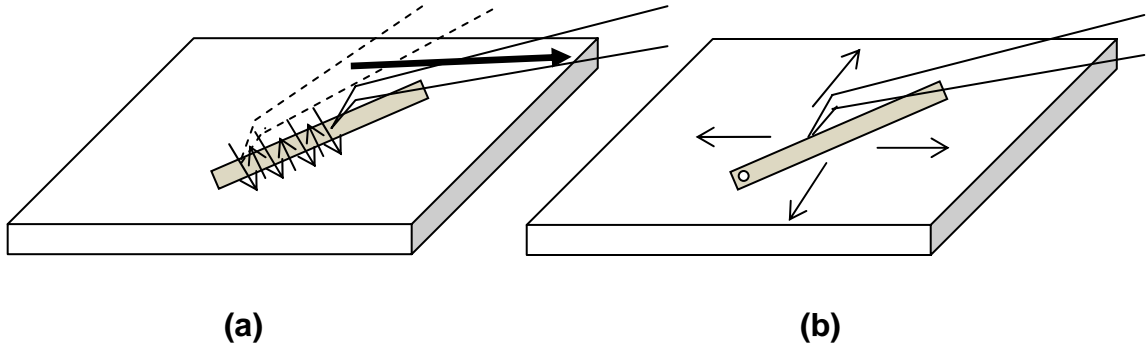


Figure 15 (a) Tip Scanning (b) Sample Scanning.

In sample scanning operations, the e-beam from the SEM can be fixed near to the tip and allows for a “pseudo CL” measurement of the sample as the e-beam impinge onto the scanned area of the sample and the AFM/NSOM tip maps the topography and optical response simultaneously. On the other hand, in a tip scanning operation, the e-beam of the SEM can be fixed onto a particular location, usually near or on a structure, while the AFM/NSOM tip will scan across the element to determine the effects of transport at near-field. In this way, the optical signal obtained in this manner has the spatial information on luminescence originating from a fixed point source.

2. Experimental Procedures

The main goal in the experiment is to generate electron-hole pairs in the sample with an e-beam from the SEM and scan the AFM/NSOM tip to map the intensity distribution due to recombination along the structure of interest. Nanonics AFM/NSOM set-up allows for simultaneous near-field optical collection with an e-beam and AFM to map the topography of the sample. Generally, there will be two main experiments. First, sample scanning will be done to conduct a “pseudo CL” experiment to ensure sufficient optical signal from the sample as well as to locate the elements to be studied. This is done by placing the cross-hair of the e-beam close (within the diffusion length) to the tip in the SEM with “spot mode”. Then sample-scanning will be done across the sample in a scan

window desired. Then, once these luminescent regions have been identified, tip scanning will be done to conduct the transport imaging study with the technique of NSOM. In the latter experiment, the e-beam will be incident at a point that is at a distance within the theoretical diffusion length to the nano-wire under study. Generally, the e-beam will be placed at either ends of the wire using “spot mode” in the SEM and tip-scanning will be done along the wire, either away from or towards the e-beam point.

IV. TRANSPORT IMAGING OF NANOWIRES

A. GENERAL FEATURES OF GaN NANOWIRES

Gallium Nitride (GaN) nanowires are semiconductor wires of great interest lately for its some of its unique properties. These nanowires have been known to be grown defect-free because of their ability to accommodate higher levels of strain and allow the migration of dislocations to the wire surface. As a result, the nanowires exhibit high performance properties electrically, optically and mechanically for use in many possible devices. GaN also has a large band-gap of 3.4 eV at room temperature and emits blue and UV light. Due to these properties, GaN nanowires potentially are useful in numerous applications like lasers, light-emitting-diodes (LEDs) and data storage devices. In general, GaN nanowires are grown via chemical vapour deposition (CVD) [19] or even with gas source molecular beam epitaxy (MBE) [20] The GaN nanowires growth techniques will not be discussed in great detail in this thesis, focusing instead on the development of a novel approach to characterizing the transport properties.

The GaN nanowires studied in this thesis are generally between 1 – 30 μm in length and 100 – 500 nm in diameter [21]. Figure 16 shows a SEM image of a 10 μm tapered GaN nanowire captured using a compact field emission SEM from Novex called mySEM. The aim is to characterize the transport properties of the wires through the technique of NSOM. Besides NSOM, other techniques such as CL imaging will be used to aid in the determination of other optical properties such as the material's CL spectrum prior to a NSOM measurement. The subsequent sections will describe the experiments and results obtained.

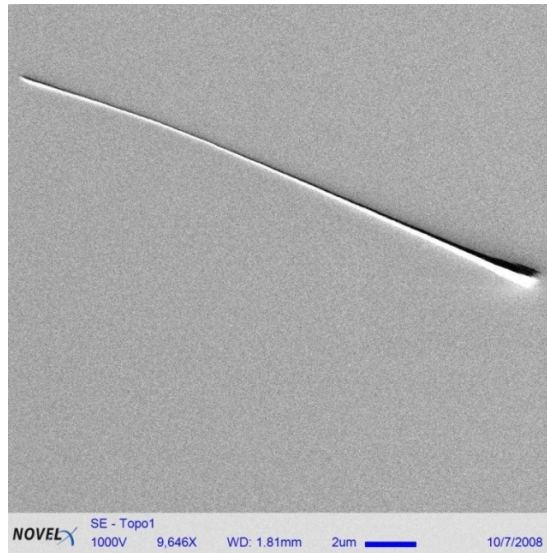


Figure 16 SEM Image of a 10 μm Tapered GaN Nanowire.

B. CL IMAGING OF GAN NANOWIRES

1. Panchromatic CL Imaging

As mentioned in Chapter III, CL imaging will be used to determine the CL spectra of the wires studied. In Figure 17 are simultaneously acquired SEM and CL images of a pair of GaN nanowires obtained using panchromatic mode CL imaging. They are 20-30 μm in length and emit light relatively well.

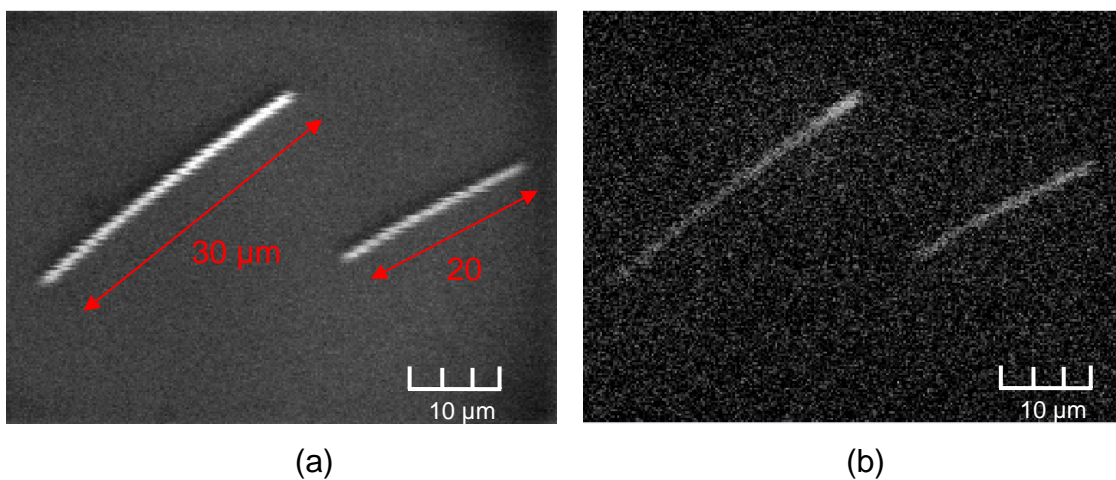
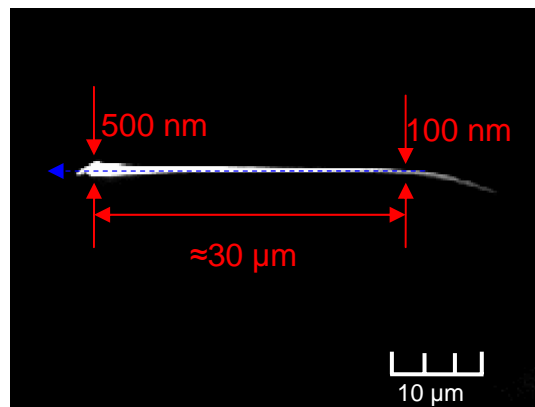
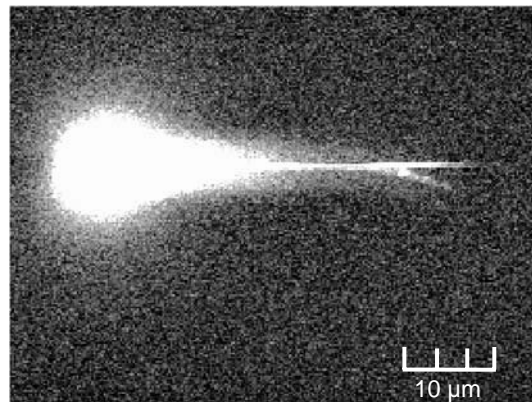


Figure 17 (a) SEM Image of a Pair of GaN Nanowires; (b) Panchromatic CL Image of the Same Wires.

Upon confirming the primary luminescent behaviour of GaN nanowires, operating the CL system in 'spot-mode' will allow for the mapping of the intensity of luminescence along a wire with a moving excitation source along a defined path on the wire. Figure 18 shows a panchromatic CL image using "spot mode" of a 30 μm GaN nanowire at 2500X and the blue line indicates the direction of the excitation source. It is significant to note that the amount of luminescence emitting from the broad end of the wire is extremely high (in order of ~ 1000 times higher) compared to the narrow end of the wire. The relative intensities of luminescence are shown in the graph in Figure 19.



(a)



(b)

Figure 18 (a) SEM Image of a 30 μm GaN Nanowire; (b) Panchromatic CL Image of the Same Wire.

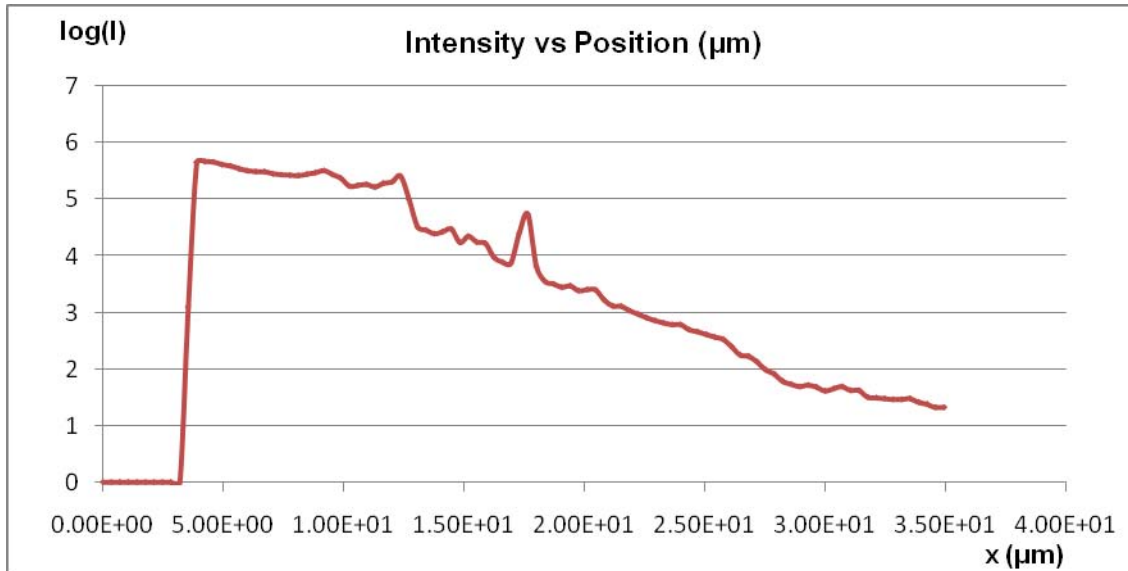


Figure 19 Spatial Variation of Luminescence from GaN Nanowire in “Spot Mode” in Panchromatic Mode.

2. Monochromatic Intensity Mapping of Nanowire in ‘Spot-Mode’

After capturing the images of the wires in panchromatic mode, it is clear that the intensity of the CL emission varies strongly along length of the wire. However, additional information can be obtained by measuring spatial variation at various emission wavelengths. An experiment is conducted for an automatic scanning spectrometer to change the wavelength selected by the monochromator and measured the intensity of luminescence as a function of wavelength. Figure 20 shows the results obtained from the measurement and it can be deduced that 360 nm is the band-edge luminescence wavelength based on the 1st and 2nd order intensities peaks at 360 nm and 720 nm respectively. 550 nm and 660 nm are observed to be the peak wavelengths associated with mid-gap recombination.

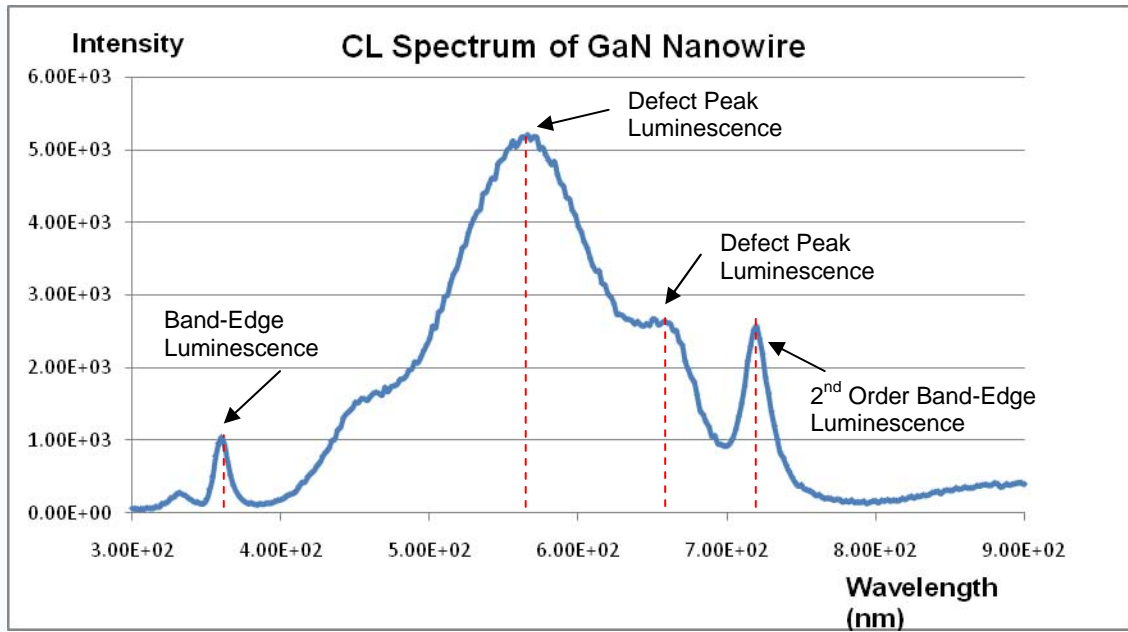


Figure 20 CL Spectrum of GaN Nanowire.

Since the peak wavelengths of the GaN nanowire emission are specifically 360 nm, 550 nm and 660 nm, operating the CL system in monochromatic collection at these wavelengths will allow the independent mapping of the band edge and defect intensity of luminescence along the wire. Figures 21, 22 and 23 below show the SEM and monochromatic CL image of a 30 μm GaN nanowire at 360 nm, 550 nm and 660 nm respectively. It is obvious (from Figure 24, 25, 26) that the CL intensity decreases as the diameter of the wire gets narrower and the intensity of luminescence at 550 and 660 nm are higher than the band-edge luminescence.

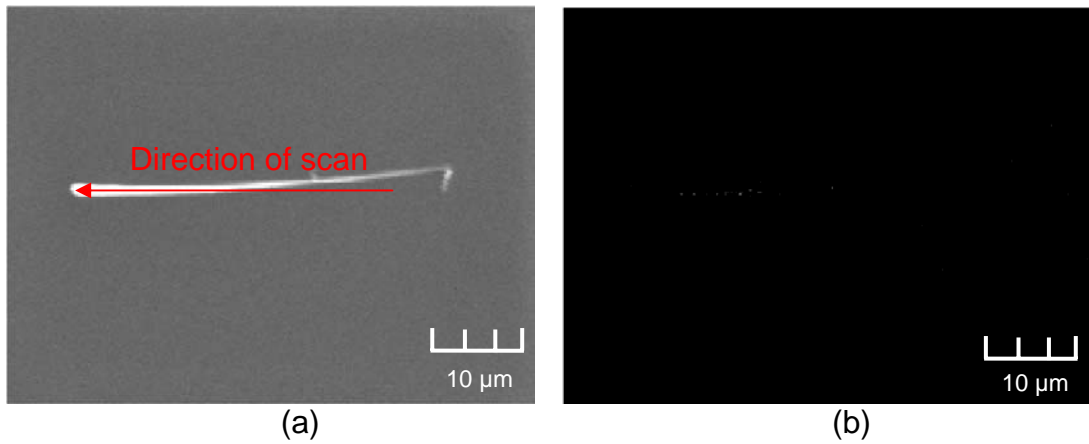


Figure 21 (a) SEM Image of a 30µm GaN Nanowire; (b) Monochromatic CL Image at 360nm.

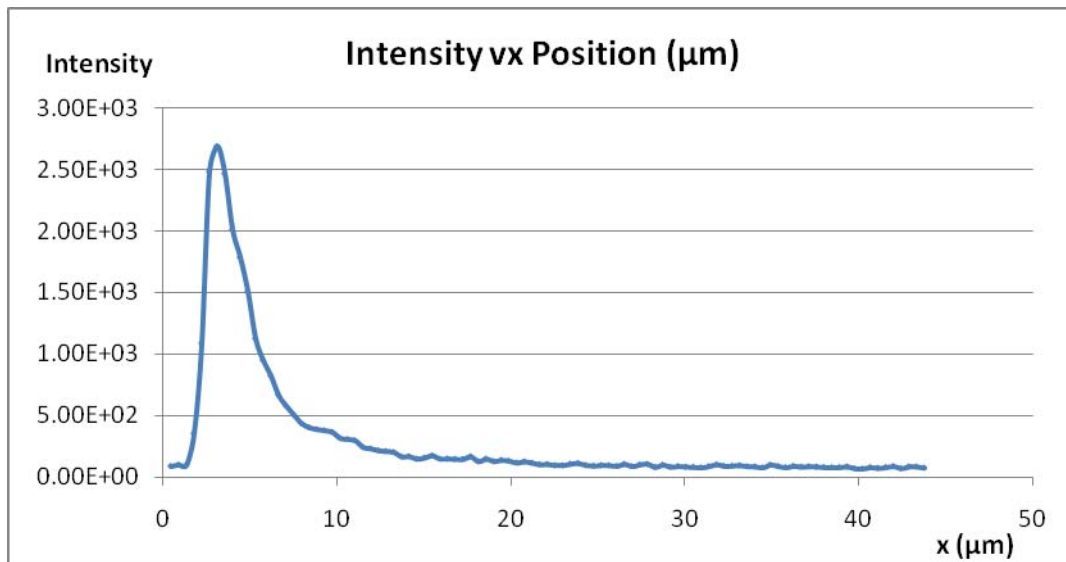


Figure 22 CL Intensity Map of GaN Nanowire in "Spot Mode" for $\lambda = 360$ nm.

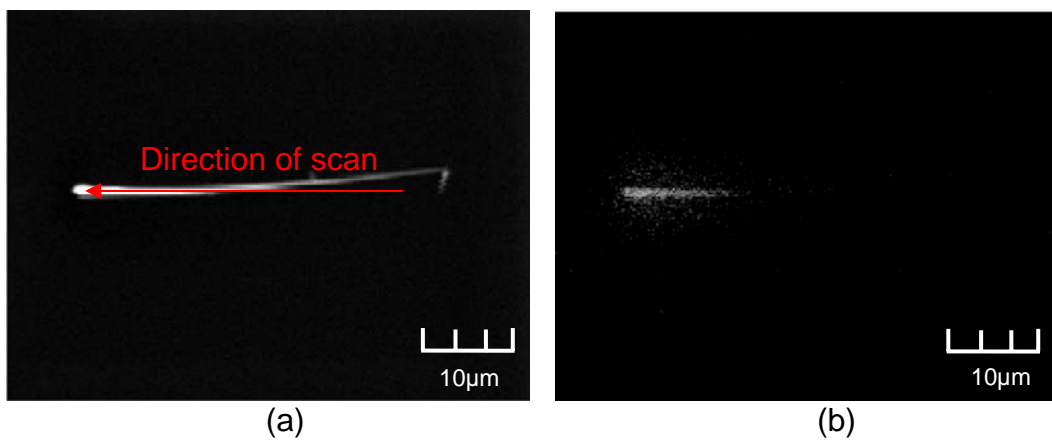


Figure 23 a) SEM Image of a 30 μm GaN Nanowire; (b) Monochromatic CL Image at 550 nm.

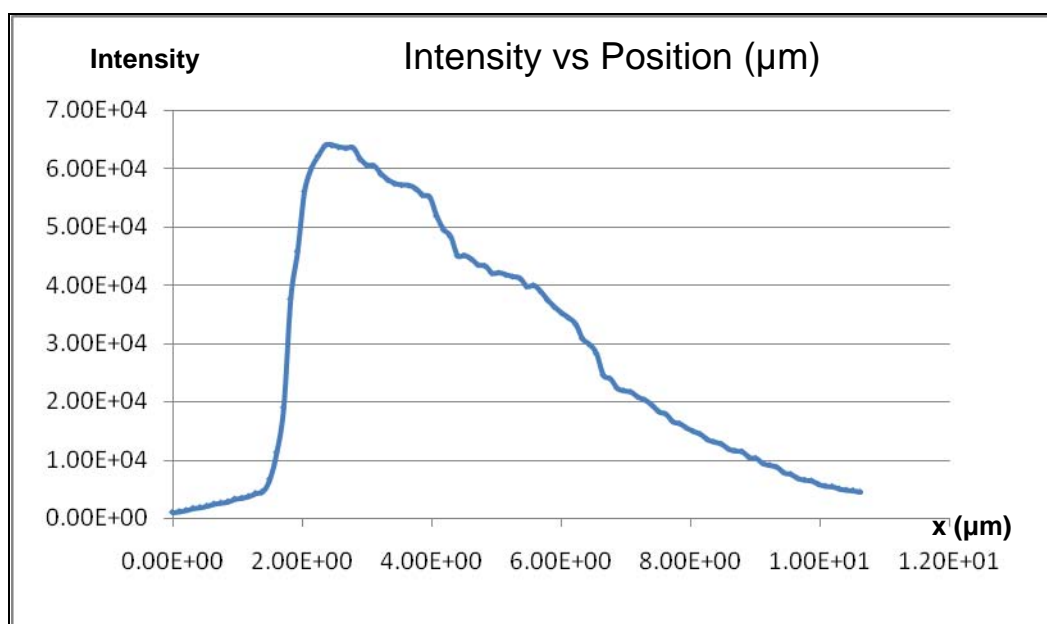


Figure 24 CL Intensity Map of GaN Nanowire in "Spot Mode" for $\lambda = 550$ nm.

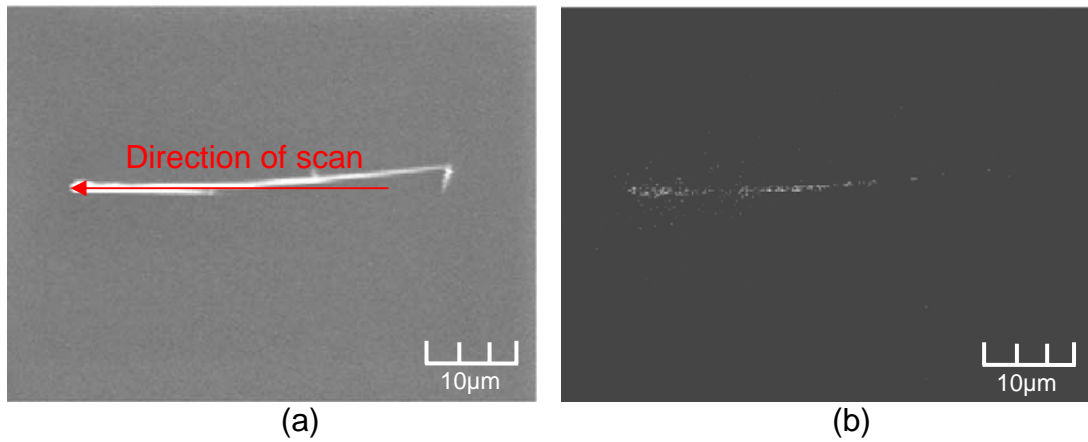


Figure 25 a) SEM Image of a 30 μm GaN Nanowire; (b) Monochromatic CL Image at 660 nm.

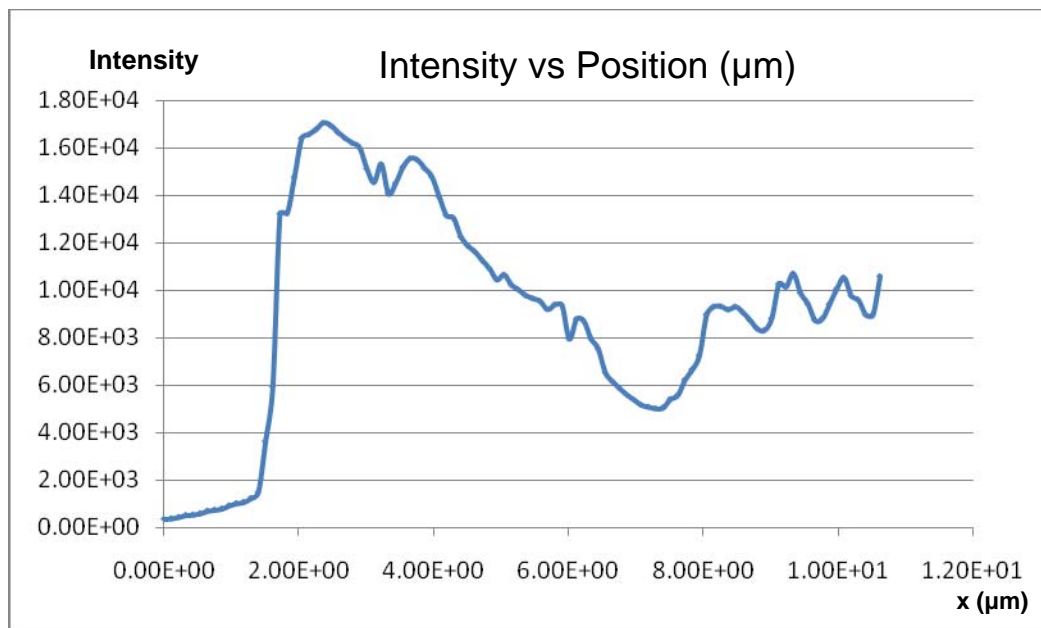


Figure 26 CL Intensity Map of GaN Nanowire in “Spot Mode” for $\lambda = 660$ nm.

Previous studies by I. Shalish et al., [22] have shown experimentally that in nanowires like ZnO, the relative strength of band-edge photoluminescence peak increases with the diameter of the wires. Figure 27 shows the photoluminescence spectra obtained from ZnO nanowires of three different sizes (100 nm, 240 nm and 540 nm in diameter). The band-edge photoluminescence occurs at 3.3 eV, with a below-band-gap peak at about 2.2 eV. It was clear that

the nanowires of approximately 100 nm in diameter showed a very much weaker band-edge emission vis-à-vis wires with diameters of around 540 nm.

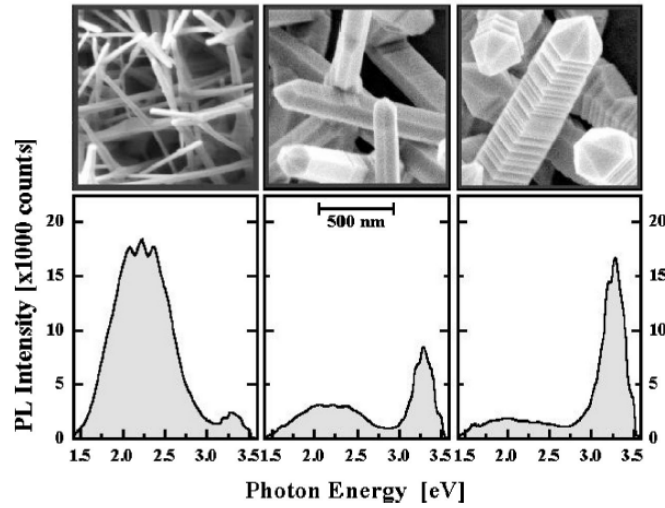


Figure 27 Photoluminescence Spectra Obtained from ZnO nanowires of Three Different Sizes [from 22].

This phenomenon has been obtained experimentally in the CL results obtained at various wavelengths. At all the peak wavelengths of 360 nm, 550 nm and 660 nm, the CL intensity maps obtained from the GaN nanowire clearly indicate that the narrower end of a GaN nanowire produces a very much weaker emission vis-à-vis the broader end of the wire at all three wavelengths.

C. AFM/NSOM RESULTS

Hundreds of AFM and NSOM scans have been done throughout this thesis work. Below are some key experimental results leading to measurement of the transport properties of GaN nanowires when a fixed e-beam source impinged at one end of the wire and the tip scanned across/along the wire to image the transport of the charge generated at the source point. Scans were done on GaN nanowires of various dimensions and from the relationship below, the effective minority carrier mobility, μ , can be estimated using the experimental results obtained for minority carrier diffusion length, L_d , in 1-dimension:

$$I \propto e^{-x/L_d}$$

1. PL-NSOM Experiment on GaAs Heterostructure

A PL-NSOM experiment has been done at Nanonics Pte Ltd in Jerusalem, Israel, to demonstrate the concept behind transport imaging with NSOM collection. A 532 nm laser light source of $1\mu\text{m}$ spot size was used as the excitation source for NSOM measurement on a GaAs double heterostructure of a sample with nanobowties. The laser spot was placed on the GaAs layer about $5\mu\text{m}$ away from an Au strip and NSOM is scanned across the laser beam spot with a $15\mu\text{m}$ by $15\mu\text{m}$ scan window. Figure 28 shows the NSOM image from this experiment. The ditch in the diffusion profile image was caused by the blocking of laser beam by the NSOM probe as the probe moved beneath the laser beam across the fixed point. This is the first NSOM image that captures the 2D diffusion effect in a luminescent material at near-field.

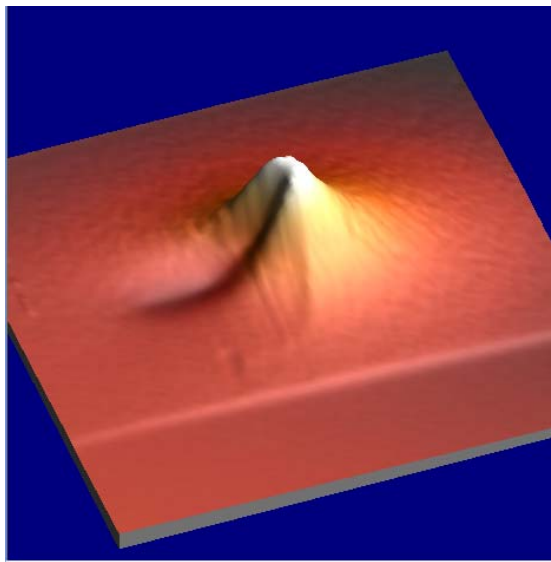


Figure 28 NSOM Image of a 15-by-15 μm Scan which Shows the 2D Diffusion Effect from the PL Fixed Spot.

2. AFM/NSOM Experiment on GaN Nanowires

After verifying the optical emission properties of GaN nanowires using the CL system, NSOM is used to determine the transport properties. Figure 29 shows the AFM, NSOM and luminescence profile of the nanowire studied

respectively. A probe of 200 nm aperture was used to conduct the AFM/NSOM scan on a 5 μm GaN nanowire at 10,000X, 3×10^{-9} A probe current, 20.0 kV accelerating voltage over a 10 μm by 10 μm scan window.

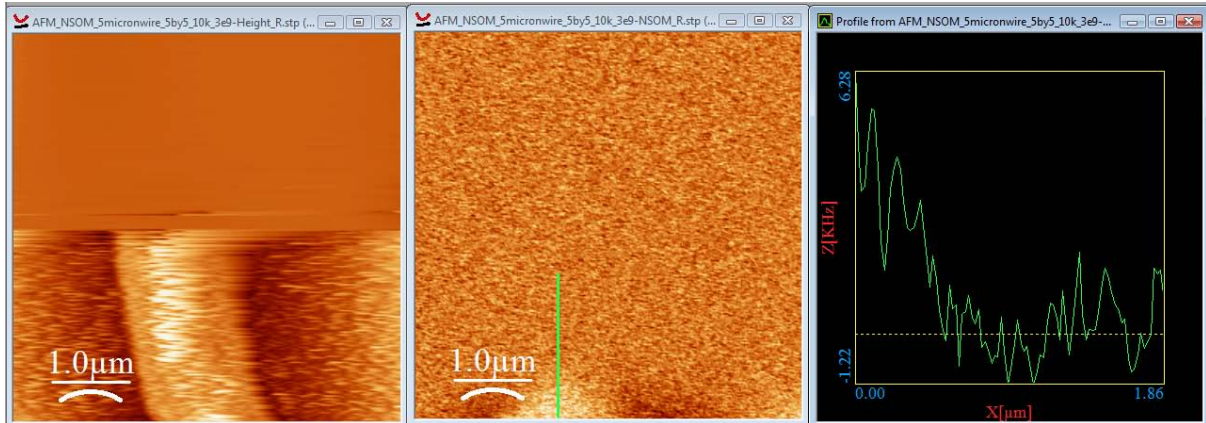


Figure 29 AFM Image, NSOM Image and Luminescence Profile of a 5 μm GaN Nanowire.

Figure 30 shows the AFM, NSOM and phase images of a 10 μm nanowire studied respectively, while Figure 31 shows the luminescence profile measured across the green line shown in Figure 30. A 3D NSOM representation is shown in Figure 32 as part of the topography of the nanowire. A probe of 200 nm aperture was used to conduct the AFM/NSOM scan at 9,000X, 1×10^{-8} A probe current, 20.0 kV accelerating voltage over a 10 μm by 10 μm scan window.

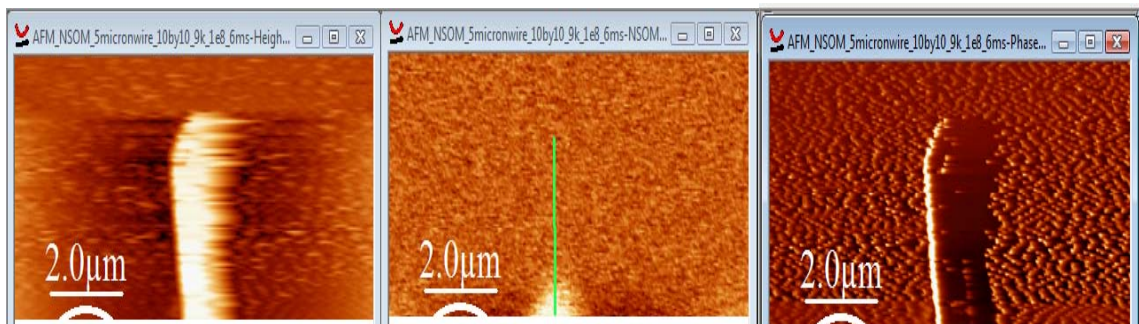


Figure 30 AFM, NSOM and Phase Image of 10 μm GaN Nanowire.

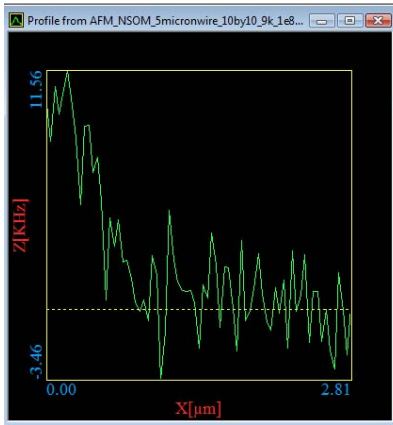


Figure 31 The Luminescence Profile of the 10 μm GaN Nanowire as Measured across the Green Line Shown in Figure 30 above.

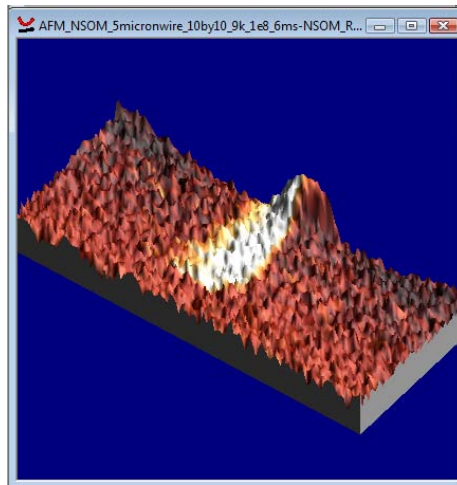


Figure 32 3D Interpretation of NSOM Signal Superimposed on the Topography of the Wire 550 nm.

Figure 33 shows the AFM, NSOM and luminescence profile of a different 5 μm nanowire studied respectively. The AFM/NSOM scan was done at 9,000X, 1×10^{-8} A probe current, 20.0 kV accelerating voltage over a 10 μm by 10 μm scan window.



Figure 33 NSOM on 5 μm GaN Nanowire, 10-by-10 μm Scan, at 1×10^{-8} A, 20.0 kV, 9000X.

It is consistent that the luminescence intensity decreases along the wire due to the short diffusion length of the material. However, we have to determine if the measured NSOM signal reflects the transport characteristics. This can be proven by determining the effective minority carrier mobility of the GaN nanowires. Figure 34 shows the semi-log plot of the luminescence intensity of the above measured GaN nanowire which displayed a linear relationship to:

$$I \approx e^{-x/L_d}$$

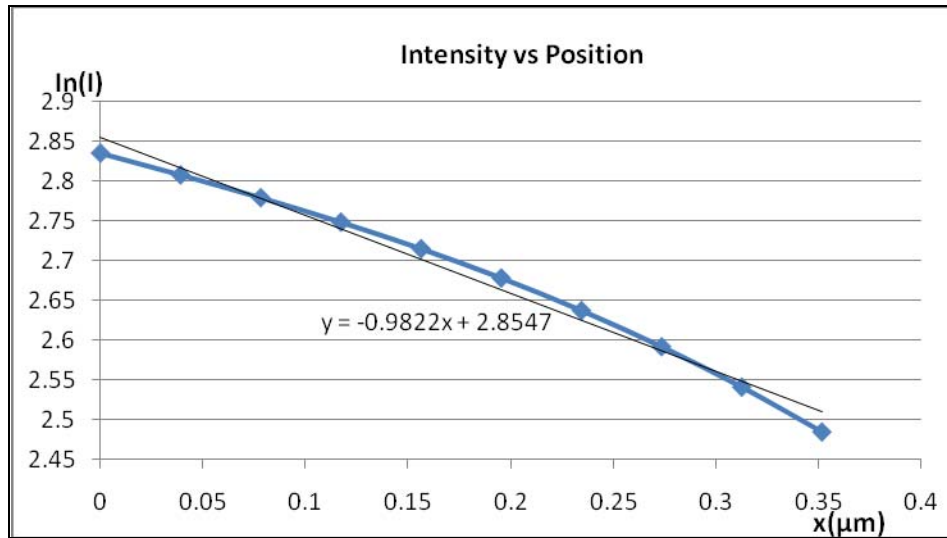


Figure 34 Semi-Log Plot of the Luminescence Intensity versus Distance for a 5 μm GaN Nanowire.

The linear regression line constructed for the linear part of the exponentially decaying optical signal obtained from NSOM scan yielded a slope of $-0.98 \mu\text{m}^{-1}$. $1/\text{slope}$ translates to the diffusion length, L_d , of $\sim 1.0 \mu\text{m}$.

Figure 35 shows the profile measurement of another 10 μm GaN nanowire and Figure 36 shows the semi-log plot of its luminescence intensity at 7,000X, 3×10^{-9} A probe current and 20.0 kV accelerating voltage.

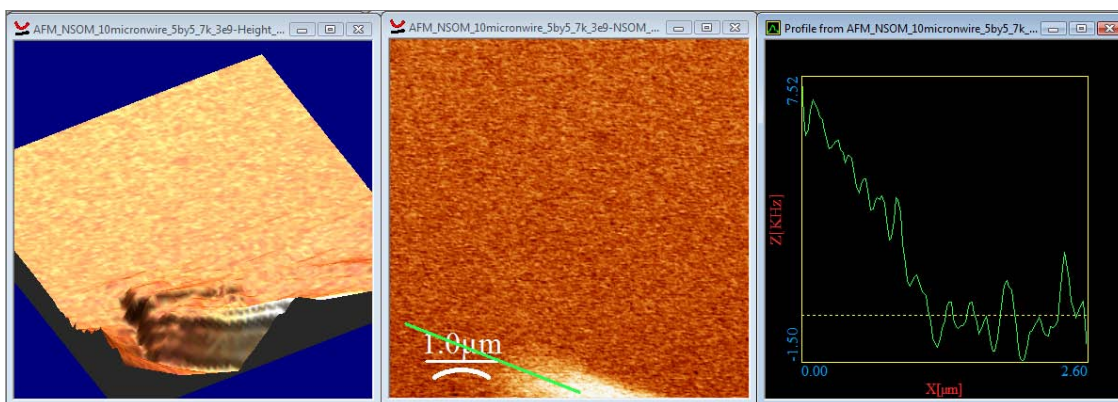


Figure 35 Profile from a 5-by-5 μm AFM/NSOM Scan of a 10 μm GaN Nanowire.

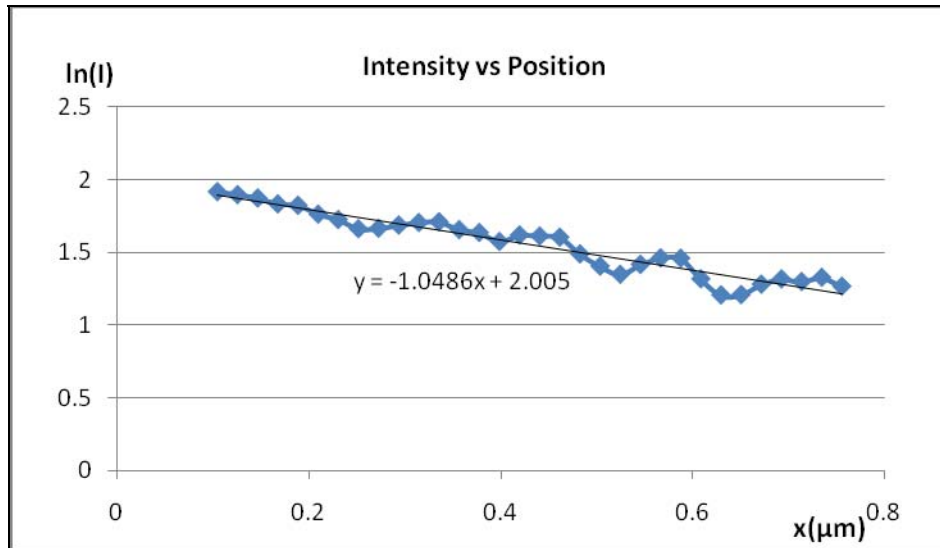


Figure 36 Semi-Log Plot of the Luminescence Intensity versus Distance for a 10 μm GaN Nanowire.

The linear regression line constructed for the linear part of the optical signal obtained from NSOM scan yielded a slope of $-1.0 \mu\text{m}^{-1}$. $1/\text{slope}$ translates to the diffusion length, L_d , of $\sim 1.0 \mu\text{m}$.

Another set of experiments were done using a probe of a larger aperture (250 nm) and it was observed that the measured diffusion lengths were slightly longer compared with the experiments conducted using a smaller aperture (200 nm). Figure 37 shows the AFM image, NSOM image and the luminescence profile measured on the narrow end (~ 100 nm in diameter) of a 15 μm GaN nanowire. Figure 38 shows the semi-log plot of the intensity profile.

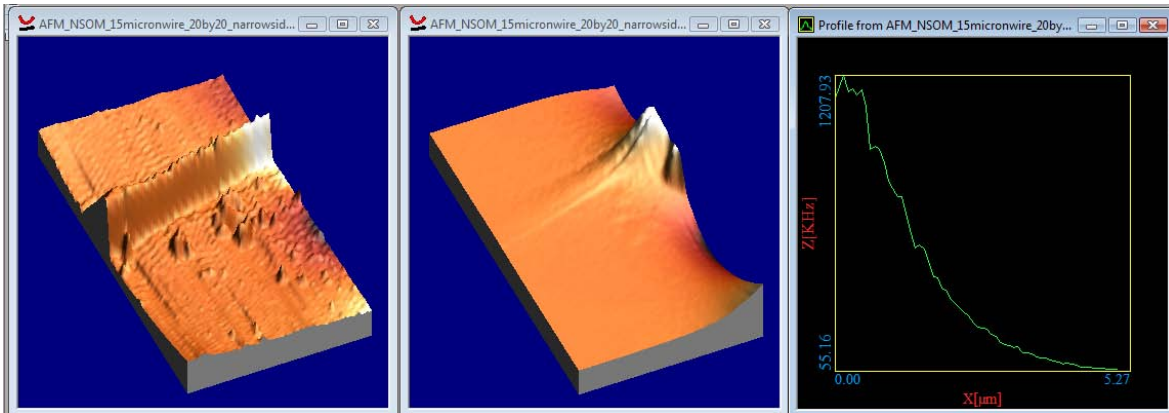


Figure 37 Profile of a 20-by-20 μm AFM/NSOM Scan of a 15 μm GaN Nanowire at its Narrow End (~ 100 nm).

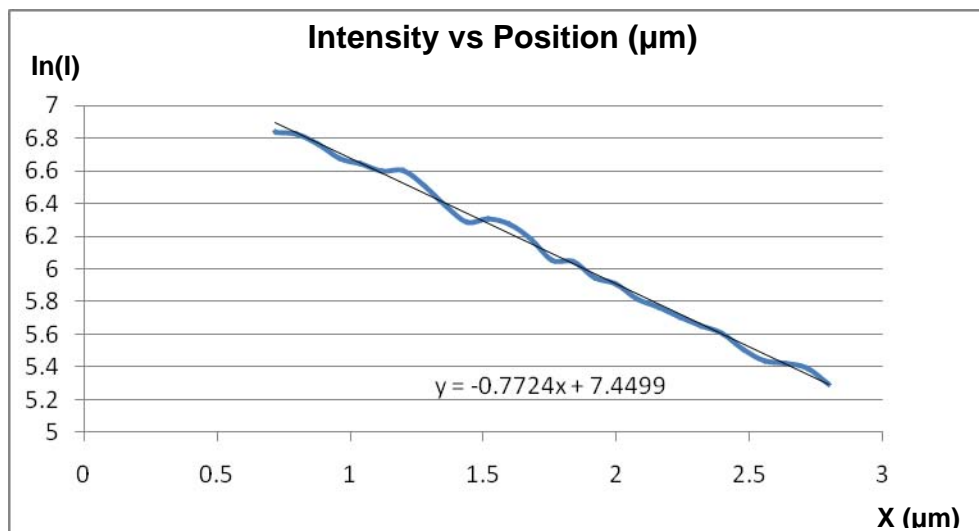


Figure 38 Semi-Log Plot of the Luminescence Intensity versus Distance for a 10 μm GaN Nanowire at its Narrow End (~ 100 nm).

The linear regression line constructed for the linear part of this exponentially decaying optical signal obtained from NSOM scan yielded a slope of $-0.7724 \mu\text{m}^{-1}$. $1/\text{slope}$ translates to the diffusion length, L_d , of $\sim 1.3 \mu\text{m}$.

Similarly, the same set of experiment was done on the broad end of the same wire and Figure 39 shows the AFM image, NSOM image and the

luminescence profile measured on the broad end (~500 nm in diameter) of a 15 μm GaN nanowire. Figure 40 shows the semi-log plot of the intensity profile.

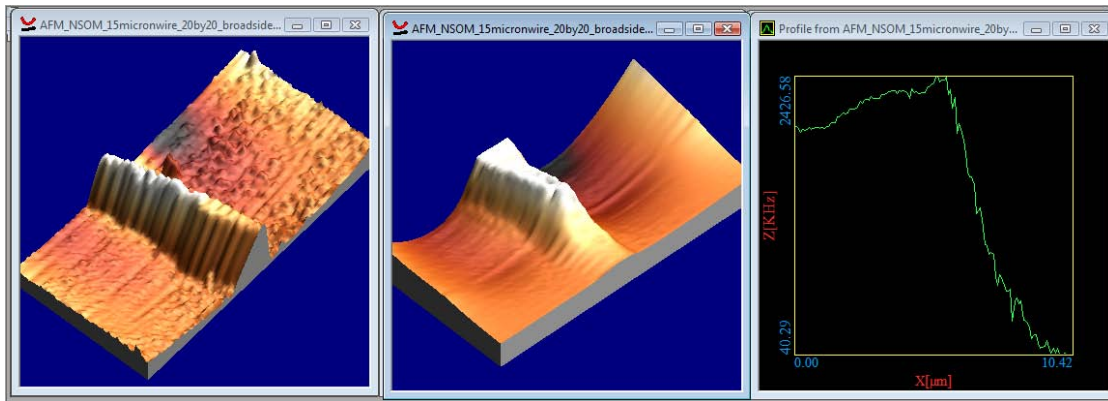


Figure 39 Profile of a 20-by-20 μm AFM/NSOM Scan of a 15 μm GaN Nanowire at its Broad End (~500 nm).

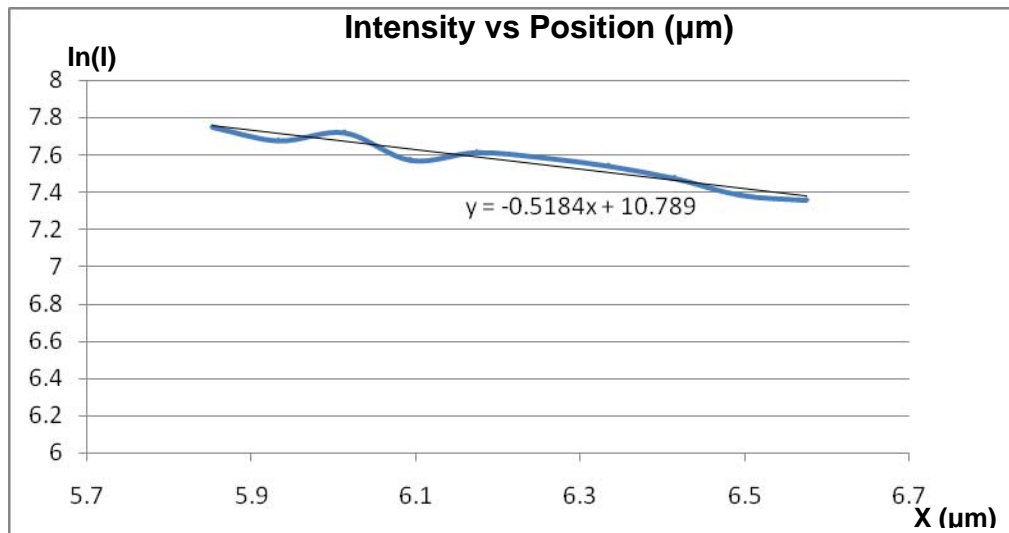


Figure 40 Semi-Log Plot of the Luminescence Intensity versus Distance for a 10 μm GaN Nanowire at its Broad End (~500 nm).

The linear regression line constructed for the linear part of this exponentially decaying optical signal obtained from NSOM scan yielded a slope of $-0.5184 \mu\text{m}^{-1}$. $1/\text{slope}$ translates to the diffusion length, L_d , of $\sim 1.9 \mu\text{m}$.

The results showed that slightly longer diffusion lengths were obtained from the experiments done using a probe of a larger aperture diameter (250 nm). It is possible that luminescence enhancement along the wire, which acts like a waveguide, could have allowed the guiding of light further along the wire. It is also possible, however, that longer wires have higher quality, and longer diffusion lengths, due to their longer growth time.

It is known that the diffusion length has the following relationship with the carrier mobility, μ and lifetime, τ :

$$L_d = \sqrt{\frac{kT}{e} \mu \tau}$$

From the approximated L_d of $1\mu\text{m}$ obtained from the experimental results, and assuming τ to be approximately 1×10^{-9} s as extracted from the results of time-resolved photoluminescence (PL) from relaxed and strained GaN nanowires [23], the calculated μ is approximately $385 \text{ cm}^2/\text{Vs}$. This value is very close to the calculated effective majority carrier mobility of $386 \text{ cm}^2/\text{Vs}$ from the experimental data obtained in the study of space-charge-limited current in GaN nanowires by A.A. Talin et al., [24].

Additionally, experimental results from a study by A. H. Chin et al., [25] showed that among the two types of GaN wires, a-axis $\langle 1010 \rangle$ and c-axis $\langle 0001 \rangle$ wires, a-axis wires exhibit a blue-shifted luminescence at around 310-350 nm, while the c-axis will exhibit band-edge peak luminescence between 350-390 nm. The lifetime that this paper has measured for a-axis GaN wires which are blue-shifted had a longer life-time of around 1 – 5 ns while c-axis wires had a lifetime of ~ 100 ps. The measurements in this study by A.H. Chin et al., were made on ~ 20 nm (diameter) wires. Cross-referencing to the time-resolved photoluminescence (TRPL) study done by [23], GaN nanowires of ~ 20 nm in diameter should yield a lifetime on the order of < 0.1 ns. This range of lifetime will

match with c-axis GaN wires discussed in [25]. The results obtained for diffusion length as well as the calculated carrier mobility in this thesis clearly are consistent with the findings of both [23], [25].

THIS PAGE INTENTIONALLY LEFT BLANK

V. INITIAL INVESTIGATIONS ON AU NANOBOWTIES

A. GENERAL FEATURES OF AU NANOBOWTIES

Nanowires are just one of the numerous nanostructures that attract immense research interest due to broad applications in many areas of electronics, photonics and sensors. This thesis extended its scope beyond nanowires to investigate the possible optical enhancement properties of Au nanobowtie structures. Figure 41 shows the actual sample that was studied in this thesis with an array of 20 nm thick Au nanobowties (200 nm in size per pair with varying gap distance of 0-50 nm) fabricated on a GaAs double heterostructure and Figure 42 shows a pair of nanobowties in high-magnification.

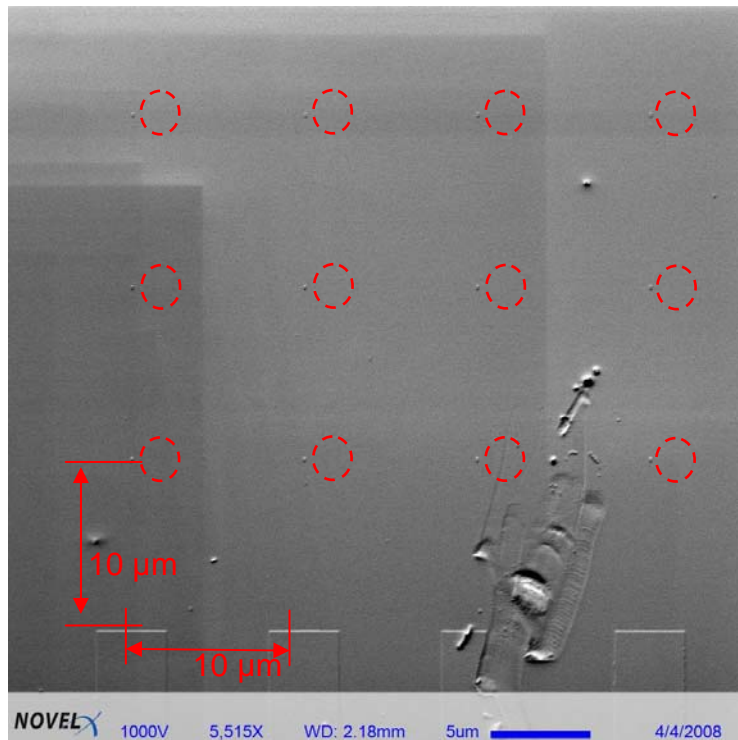


Figure 41 Au Nanobowties Array Fabricated on a GaAs Heterostructure with Au Strips of 10 μm Pitch to Demarcate the Locations of Nanobowties at 10 μm Intervals along Each Strip (Image Captured Using NovelX mySEM). This is the Actual Sample Used for this Thesis Work.

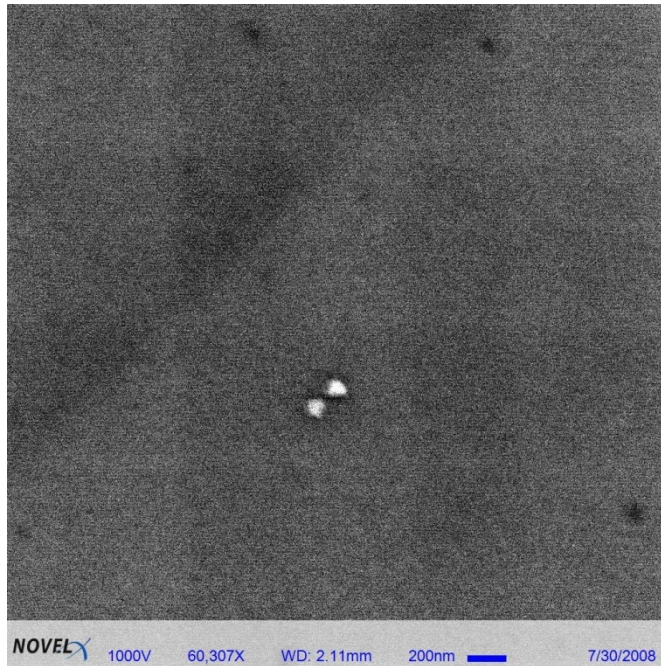


Figure 42 A Pair of Au Nanobowties with 50 nm Gap (Image Captured Using NovelX mySEM).

Based on the theory that electric field can be enhanced by either plasmon resonance or sharp edges at reduced dimensions a study by Grober et al., [26] demonstrated the field enhancement phenomenon between the nanotriangles of a pair of nanobowties for microwaves frequencies. A. Sundaramurthy et al., [27] extended this finding through the construction of a physical model based on current distribution around the nanobowtie antennas to demonstrate the variation of resonant wavelength with the gap between the bowtie elements to the visible range. To reach visible frequencies, the nanotriangles have to be in dimensions <100 nm. From their finite-difference time-domain (FDTD) simulations, very strong optical intensity enhancement was predicted to occur between the gaps of the nanobowties. This optical property makes nanobowties useful in potential applications like high-resolution imaging [28], which is in high demand in the field of nanotechnology today. To date, however, direct experimental imaging of this enhanced emission in the near-field has been limited.

B. AFM OF AU NANOBOWTIES

The same experimental set-up and procedures for the measurement of GaN nanowires were also used in the study of Au nanobowties. AFM was first used to locate and measure the topography of the nanobowtie elements prior to any NSOM optical collection. Figure 43 shows one of the earliest AFM image (with a very clean substrate) obtained with 5 μm by 5 μm scan using a 250 nm diameter AFM/NSOM probe. As the diameter of the probe was very much bigger than the nanotriangles and the gap between the nanobowties, this image is considered a good AFM image.

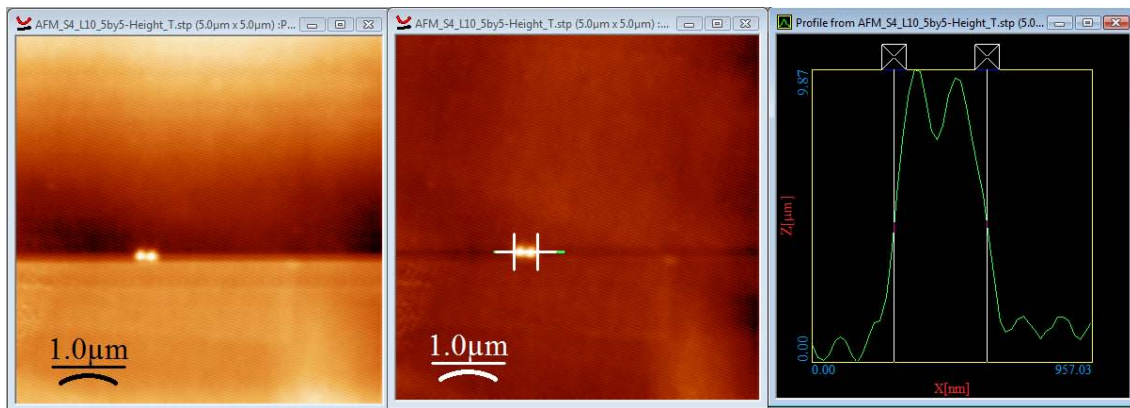


Figure 43 AFM Image of a Pair of Au Nanobowtie and its Profile Measurement.

Figure 44 shows another pair of nanobowtie with a 45 nm gap measured by an integrated AFM/NSOM probe of 250 nm diameter and its corresponding topography profile. The surrounding particles around the nanobowties are dust and dirt particles.

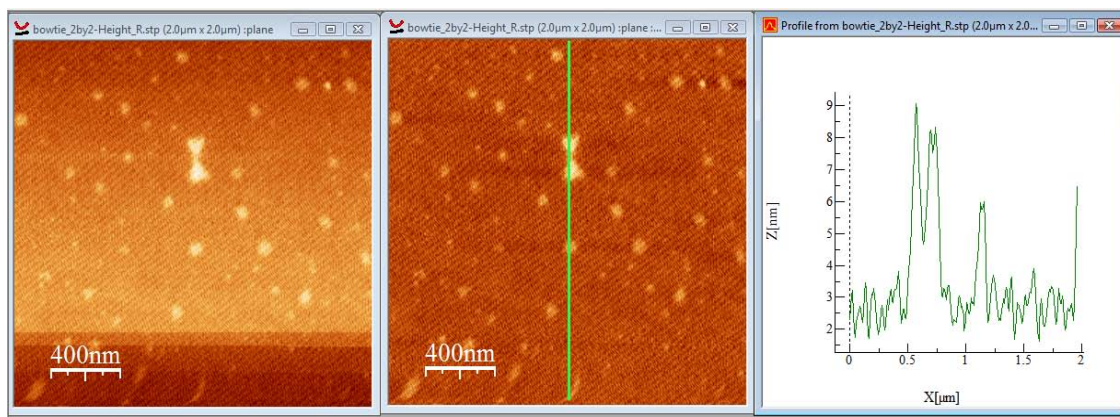
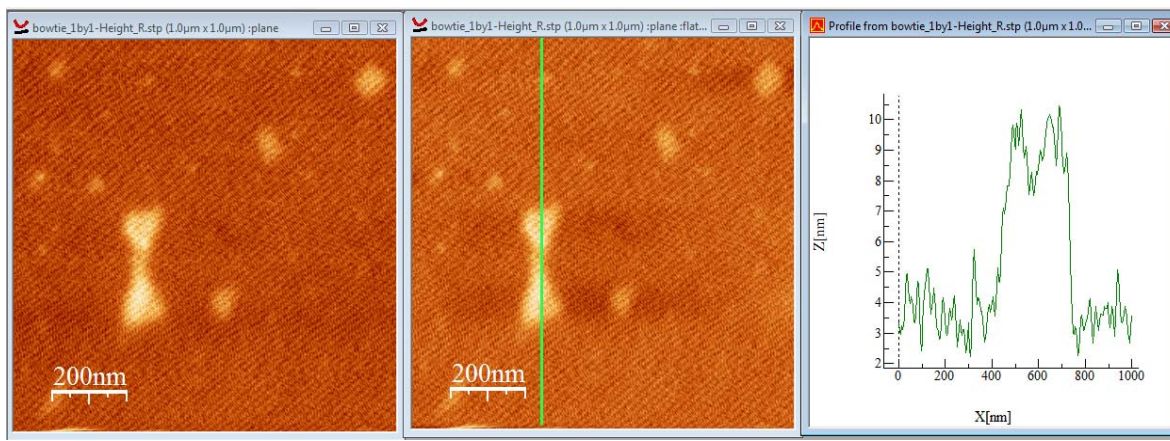
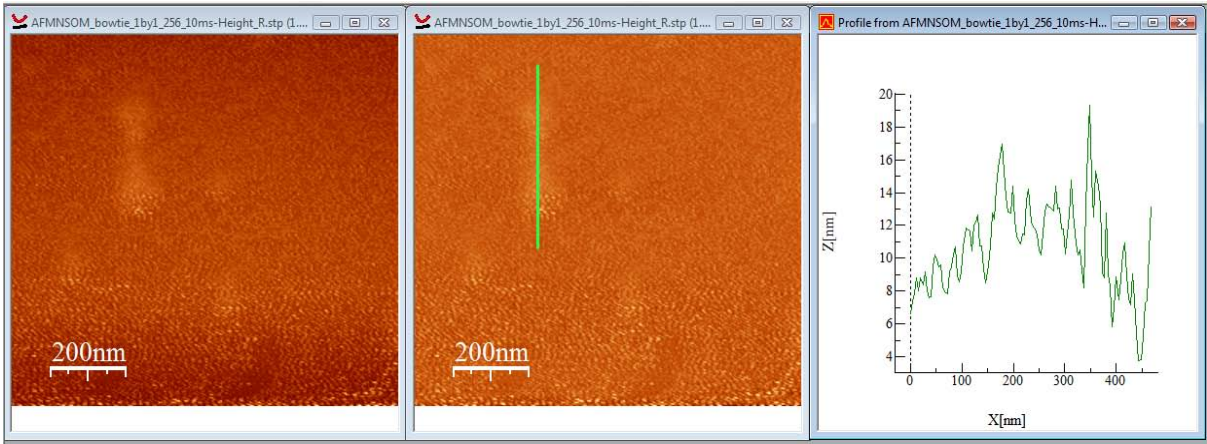


Figure 44 A Pair of Au Nanobowties with a 45 nm Gap Measured by AFM and its Corresponding Topography Profile.

A common problem in high magnification AFM/NSOM measurement in this thesis work is the charging effect between the probe and the sample that causes drifting motion of the sample. Although the charging effect can be minimized by grounding the sample surface, it is not negligible at the nano-scale measurement. An example of how the “drifting effect” results in poorer resolution is shown in Figure 45 below.



(a)



(b)

Figure 45 1 μm by 1 μm AFM Scan of a Pair of Nanobowties with (a) SEM Beam Off and (b) SEM Beam On.

In general, integrated AFM/NSOM probes are larger in aperture sizes and they range from 100 nm to 300 nm in diameter. A trip was made to Agilent Technologies to compare AFM measurements of the same Au nanobowties sample with AFM probes of relatively smaller diameters. A 10 nm AFM probe was used and Figure 46 clearly shows a better-resolved AFM image as compared to an integrated AFM/NSOM probe.

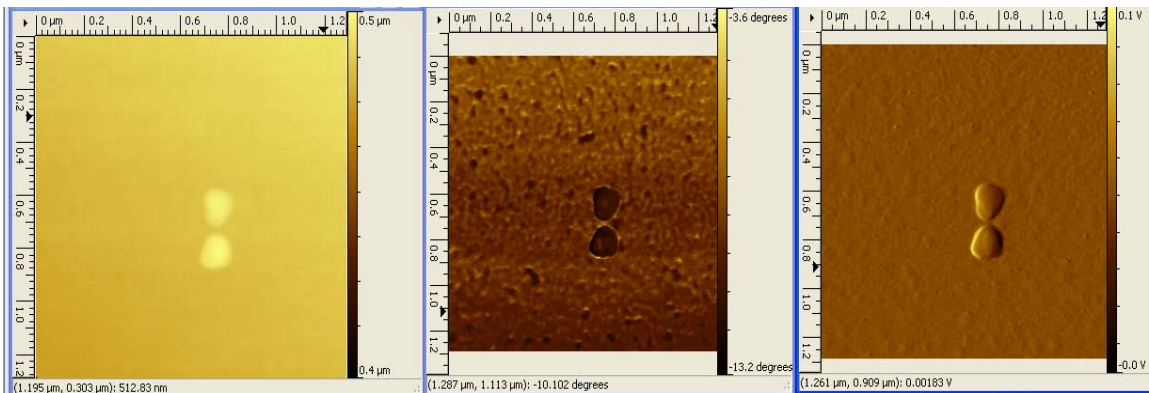


Figure 46 A Pair of Au Nanobowties Measured with a 10 nm AFM Probe.

C. NSOM OF AU NANOBOWTIES

The initial objective of this study was to determine any optical enhancement effects in the gap between any pair of Au nanobowties. This measurement can be done in near-field by scanning an integrated AFM/NSOM probe across the gap of the nanobowties while placing a fixed e-beam source near to the gap. As the diffusion length of the GaAs epitaxial layer is less than $3\ \mu\text{m}$ [3], it is important that the e-beam spot be placed within this distance from the gap in order to create luminescence at the location of the nanobowties gap and observe the enhancement effects in the gap, if any. Although NSOM is the ultimate experiment to determine the optical enhancement effects of the Au nanobowties, the common problem of probe-sample charging in the SEM caused a “drifting effect” of the sample to render all NSOM measurement ineffective. Figure 47 below illustrates schematically how the “drifting effect” hinders the NSOM measurement across the Au nanobowties.

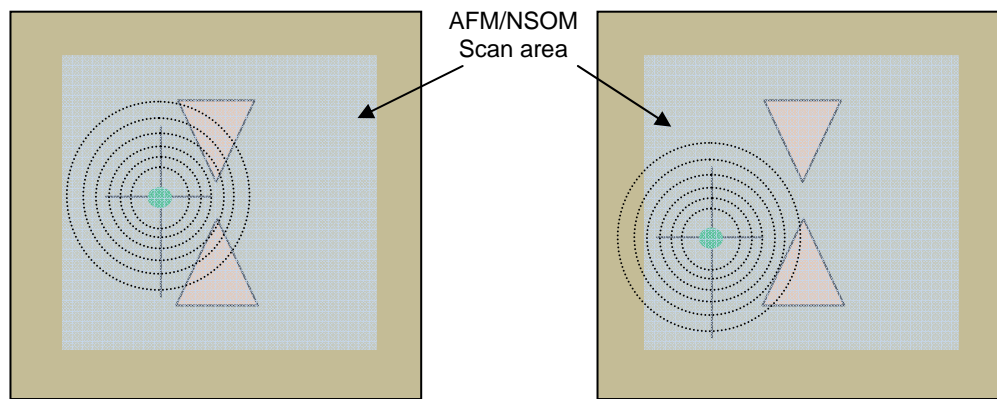


Figure 47 (a) The E-beam was Placed (with a Cross-hair) at Close Proximity to the Gap of the Nanobowtie so as to Determine Any Optical Enhancement Effects; (b) The Location of the E-beam after a Complete Scan will not have the Proximity for Optical Field to Reach the Gap.

It is deduced that as the NSOM scans were completed with the e-beam spot moving away from the gap, the minority carrier diffusion effect of GaAs will not be able to reach the gap for any significant measurements. No enhanced emission was observed in multiple attempts.

D. CHALLENGES FOR NSOM OF AU NANOBOWTIES

As mentioned in the earlier section, the main challenges of this work are to be able to: 1) bring the e-beam spot ($\sim 1 \mu\text{m}$ in diameter) within $3 \mu\text{m}$ to the gap of a pair of Au nanobowtie, and 2) ensure that the e-beam spot is fixed onto a point where the experiment desired without the “drifting effect” caused by probe-sample charging by innovatively grounding the probe. Until these technical challenges are overcome, NSOM measurement of any nanostructures as small as these Au nanobowties will be a great challenge with the current experimental set-up. An additional alternate approach that could be investigated would be to use a forward-biased solar cell structure to illuminate the bowtie gap and collect the spatially resolved emission in the near-field, removing the role of the electron beam to generate the light.

THIS PAGE INTENTIONALLY LEFT BLANK

VI. CONCLUSIONS AND SUGGESTIONS FOR FURTHER RESEARCH

A. CONCLUSION

This thesis has achieved its aims to image the optical transport properties of GaN nanowires that range from 1 – 30 μm in length and 100 – 500 nm in diameters using the technique of NSOM. The unique set-up of performing AFM and NSOM operations in a SEM to collect spatially resolved luminescence and image transport on nano-scale structures, particularly nanowires, in 1-D, has allowed direct determination of transport parameters, such as minority carrier mobility and diffusion length in near-field and the results were compared in close reference to [21], [25].

This work has demonstrated significant development of a unique nano-scale imaging technique applicable to a wide range of structures through the successful experimental approach in the verification of the minority carrier diffusion length for GaN nanowires in near-field. Effects of luminescence intensity and the diameter of the nanowires have also been experimented. For the first time in this research, the author addressed numerous challenges such as the intricate NSOM technique to resolve sub-wavelength dimension measurements of the elements and determine optimized experimental parameters to compensate for the relatively low efficiency of NSOM optical collection.

An initial investigation to determine the unique transmission enhancement through Au nanobowties fabricated on GaAs substrate has been conducted with an innovative technique using NSOM with the same experimental set-up for GaN nanowires measurements. Although it was identified theoretically in past research that under linear polarizations in two orthogonal directions, the optical near fields of the bowtie aperture made in gold is able to provide a nano-scale optical enhanced spot when the incident light is polarized across the bowtie gap via the method of transport imaging, initial experimental results showed no clear

enhancement phenomenon. Part of the challenge lies in the fixing of the e-beam spot close to the Au nanobowties gap without moving, but technical limitations currently constrained the measurements.

In this thesis, the author has reported the working principles, experimental procedures, optimal process parameters and the respective imaging results for assessing the properties of the nano-devices studied in this thesis work. Recommendations for future work pertaining to the augmentation of related NSOM work will also be made to ensure the continued progress in this area of work.

B. SUGGESTIONS FOR FURTHER RESEARCH

1. Overcoming Probe-Sample Charging “Drifting Effect”

As mentioned in the earlier chapters, one of the greatest technical challenges in this work is the probe-sample charging “drifting effect” that is undesirable in NSOM and AFM measurements of nano-scale structures. One solution is to effectively find a way to ground the AFM/NSOM probe to reduce the charging effects substantially. Alternatively, a forward-biased solar cell structure can be utilized to illuminate the desired location, such as the gap of the bowtie and collect the spatially resolved emission in the near-field, removing the role of the electron beam to generate the light.

2. Investigating Secondary Effects of the Enhanced Diffusion in GaN Nanowires

It has been observed that the diffusion effect of luminescence from the GaN nanowires was larger and longer when a NSOM probe of a larger aperture was used. Although more light can be collected via a larger aperture, the diffusion length of the GaN nanowires should remain unchanged. Initial deduction to this observation is that the nanowires actually act like waveguides which could have allow the progression of light further along the wire and this could have only be collected by apertures of a certain size due to their difference in efficiency

[17]. Future work should include a quantitative study to the relationship between measured “pseudo-diffusion length” and the aperture size of the AFM/NSOM probe.

THIS PAGE INTENTIONALLY LEFT BLANK

LIST OF REFERENCES

- [1] Tevye Kuykendall, Peter J. Pauzauskie, Yanfeng Zhang, Joshua Goldberger, Donald Sirbuly, Jonathan Denlinger, and Peidong Yang, *Crystallographic alignment of high-density gallium nitride nanowire arrays*, Nature Materials, Issue 3 Vol 8, pg 524-528, August 2004.
- [2] N.M. Haegel, J.D. Fabbi, and M.P. Coleman, *Direct transport imaging in planar structures*, Applied Physics Letters, 84, 1329, 2004.
- [3] D.R. Lubber, F.M. Bradley, N.M. Haegel, M.C. Talmadge, M.P. Coleman, T.D. Boone, *Imaging transport for the determination of minority carrier diffusion length*, Applied Physics Letters, 88, 163509, 2006.
- [4] Nancy Haegel, Goon Hwee Ang, T. J. Mills, Naval Postgraduate School, Michael Tal-Madge, Fairfield University, *Optical transport imaging for the direct measure of diffusion length anisotropy*, Meeting of The American Physical Society, March 2008.
- [5] D. Kharat, H. Muthurajan, B. Praveenkumar, *Present and futuristic military applications of nanodevices*, Synthesis and Reactivity in Inorganic, Metal-Organic, and Nano-Metal Chemistry, Vol 36, 2, pp. 231-235(5), 2006.
- [6] "Smart materials for use in next generation military vehicles." The A to Z of Nanotechnology, 2 December 2004.
<<http://www.azonano.com/details.asp?ArticleID=520>> (Last accessed 12 December 2008).
- [7] "Nanotech weaponry." Center for Responsible Nanotechnology, 12 February 2004.
<http://crnano.typepad.com/crnblog/2004/02/nanotech_weapon.html> (Last accessed 12 December 2008).
- [8] B.G. Yacobi and D.B. Holt, *Cathodoluminescence microscopy of inorganic solids*, Plenum Press, New York and London, 1990.
- [9] Haegel et. al., *Direct imaging of anisotropic minority-carrier diffusion in ordered GaInP*, submitted to J. Applied Physics, October 2008.
- [10] Max Born; Emil Wolf (1997). *Principles of optics*. Cambridge University Press, ISBN 0521639212.

- [11] E.H. Synge, *A suggested method for extending the microscopic resolution into the ultramicroscopic region*, Phil. Mag. 6, 356 (1928).
- [12] E.H. Synge, *An application of piezoelectricity to microscopy*, Phil. Mag, 13, 297 (1932).
- [13] J.A. O'Keefe, *Resolving power of visible light*, Journal of the Opt. Soc. of America, 46, 359 (1956).
- [14] E.A. Ash and G. Nichols, *Super-resolution aperture scanning microscope*, Nature 237, 510 (1972).
- [15] A. Lewis, M. Issacson, A. Harootunian and A. Muray, *Development of a 500-Å spatial-resolution light-microscope. 1. Light is efficiently transmitted through gamma-16 diameter apertures*, Ultramicroscopy, Vol 13, Issue 3, Pg: 227-231 (1984).
- [16] "Learn NSOM." Nanonics Imaging Ltd. <<http://www.nanonics.co.il>> (Last accessed 12 December 2008).
- [17] P. Burgos, *Near-field scanning optical microscopy probes: A comparison of pulled and double-etched bent NSOM probes for fluorescence imaging of biological samples*, Journal of Microscopy, Vol 211, Pt 1, pp 37-47, July 2003.
- [18] D. N. Davydov, K. B. Shelimov, T. L. Haslett and M. Moskovits, Appl. Phys. Lett. 75, 1796 (1999).
- [19] J. C. Wang, S.Q. Feng, D.P. Yu, *High-quality GaN nanowires synthesized using a CVD approach*, Appl. Phys. A 75, 691–693 (2002).
- [20] K.A. Bertness, N.A. Sanford, J.M. Barker, J.B. Schlager, A. Roshko, A.V. Davydov, and I. Levin, *Catalyst-free growth of GaN nanowires*, Journal of Electronic Materials, Vol. 35, No. 4, 2006.
- [21] S. D. Hersee, M. Fairchild, A. K. Rishinaramangalam, M. S. Ferdous, L. Zhang, P. M. Varangis, B. S. Swartzentruber, A. A. Talin, *GaN nanowire light emitting diodes*, Applied Physics Letters, In press, 2008.
- [22] I. Shalish, H. Temkin and V. Narayanamurti, *Size-dependent surface luminescence in ZnO nanowires*, Physical Review B 69, 245401, 2004.
- [23] Schlager, JB Bertness, KA Blanchard, PT Robins, LH Roshko, A Sanford, NA, *Steady-state and time-resolved photoluminescence from relaxed and strained GaN nanowires grown by catalyst-free molecular-beam epitaxy*, Journal of applied physics 2008 , 103 , 124309 -124309.

- [24] A. A. Talin, F. Léonard, B. Swartzentruber, X. Wang, S. Hersee, *Unusually strong space-charge-limited current in thin wires*, Physical Review Letters, Vol: 101 Issue: 7 Pages: 076802, 2008.
- [25] Chin Alan H; Ahn Tai S; Li Hongwei; Vaddiraju Sreeram; Bardeen Christopher J; Ning Cun-Zheng; Sunkara Mahendra K, *Photoluminescence of GaN nanowires of different crystallographic orientations*, Nano letters 2007;7(3):626-31..
- [26] R. D. Grober, R. J. Schoelkopf, and D. E. Prober, *Optical antenna: towards a unity efficiency near-field optical probe*, Appl. Phys. Lett. 70, 1354 (1997).
- [27] A. Sundaramurthy, K. B. Crozier, G. S. Kino, D. P. Fromm, P. J. Schuck and W. E. Moerner, *Field enhancement and gap-dependent resonance in a system of two opposing tip-to-tip Au nanotriangles*, Phys. Rev. B 72, 165409 (2005).
- [28] P. J. Schuck, D. P. Fromm, A. Sundaramurthy, G. S. Kino, and W. E. Moerner, *Improving the mismatch between light and nanoscale objects with gold bowtie nanoantennas*, Phys. Rev. Lett. 94, 017402 (2005).

THIS PAGE INTENTIONALLY LEFT BLANK

INITIAL DISTRIBUTION LIST

1. Defense Technical Information Center
Ft. Belvoir, Virginia
2. Dudley Knox Library
Naval Postgraduate School
Monterey, California
3. Professor James H. Luscombe
Chairman, Department of physics
Naval Postgraduate School
Monterey, California
4. Professor Nancy M. Haegel
Naval Postgraduate School
Monterey, California
5. Low Chun Hong
Republic of Singapore Armed Forces
Republic of Singapore
6. Professor Yeo Tat Soon, Director
Temasek Defence Systems Institute
National University of Singapore
Republic of Singapore
7. Tan Lai Poh (Ms), Assistant Manager
Temasek Defence Systems Institute
National University of Singapore
Republic of Singapore